

Scattering of electronic waves in square and triangular lattice half-planes with monoatomic step*

Basant Lal Sharma[†]

September 4, 2019

Abstract

Scattering of electronic waves in square and triangular lattice half-planes by a step on the surface is analyzed using the nearest-neighbour tight binding approximation. The changes in lattice spacing and the transfer integral between nearest-neighbor sites near the surface are ignored. A standard application of the discrete Wiener–Hopf method leads to an exact solution of the scattering problem associated with incidence from the ‘bulk’. A far-field approximation of electronic wavefunction, as well as its graphical comparison with a numerical solution, are also provided. Natural applications and possible extensions are based on the bulk Brillouin zone for two dimensional lattice planes as well as surface energy bands for fcc crystals.

0 Introduction

The dynamics of electrons in crystalline materials has evoked enormous interest historically [11, 64, 60]. Even in present times it continues to play a fundamental role at nanoscale and pose profound challenges [144, 7, 6]; a phrase that succinctly summarizes the concomitant puzzles is ‘size effect’ [135]. However the dimensional issues have been raised since the foundations of the electron theory of metals were laid [136, 34, 35, 36, 37], and the high specific electrical resistance exhibited by thin metal films has been explained by the limitation of the electronic mean free path due to the geometry of the film [3, 135]. The surface contribution to the resistivity is attributed to surface roughness, i.e. the deviation from a perfectly plane surface. Indeed, the ubiquitous surface scattering is still elusive while it is considered to play a key role in the increase in resistivity of thin films [101, 45, 38, 130, 99], see also [74, 44].

*The support of SERB MATRICS grant MTR/2017/000013 is gratefully acknowledged.

[†]Department of Mechanical Engineering, Indian Institute of Technology Kanpur, Kanpur, U. P. 208016, India. E-mail: bls@iitk.ac.in, Phone: +91 512 259 6173, Fax: +91 512 259 7408

In 1938, based on the scattering of conduction electrons at the film surfaces, supported by early experimental data, K. Fuchs [31] formulated a theory that related decrease in thickness to the increase in electrical resistivity of thin metal films [144]. This description of the surface is strictly phenomenological and assumes that the state of the surfaces can be adequately described by the single specularly parameter p [67]. Clearly, it is not detailed enough to adhere to any specific microscopic scattering mechanism. Nevertheless, Fuchs's theory is widely applied to analyse experimental data even to this date. A convenient form of this expression for the conductivity has been given by Chambers [18] and Sondheimer [126]. From a theoretical point of view, several modifications of such model have been proposed in the literature [91, 76, 82, 125, 46, 30, 89] for each component of the total resistivity; there have been attempts to generalize the hypothesis of a *single* specularly parameter p [18, 126] to an angle-dependent specularly parameter [42, 40, 39, 146]. A number of surface scattering mechanisms have been also analyzed [59] towards reasonable theoretical discussions of an angle-dependent specularly parameter [41, 122]. It is well known that the geometrical surface roughness is one of the most important mechanisms on clean surfaces [146, 123]. In the Fuchs-Sondheimer model [31, 126] the phenomenological parameter $p = 1$ characterizes perfectly specular electron scattering while $p = 0$ means completely diffusive scattering. In practice, the degree of specular scattering at rough surfaces is determined by fitting the ab initio data to the Fuchs-Sondheimer model, for example see [51]. Other more advanced analytic models have also been proposed in later years in the general area of thin-film resistivity which take into account the quantum mechanical effects that may become prominent for extremely thin films [137, 30, 77].

The surface scattering of conduction electrons also often reduces to scattering by potential centers randomly distributed over the surface [5, 141, 142]. In the context of this paper, the classic work of Greene and O'Donnell [41] is relevant. These authors presented a detailed analysis for electron scattering from a random array of surface charges where a crucial role is played by the differential scattering probability (calculated from the scattering amplitude for one scatterer). Analogous problem holds for the rough surface of crystalline materials. Thus, in case of surface steps, as a counterpart of equation (8a) of [41], it is required that the scattered wavefunction (difference between total wavefunction and its geometric part, i.e., $\psi - \psi^g$) is obtained in the far-field for a single surface step as shown in Fig. 1 schematically. This discloses the first motivation behind the present paper where it is assumed that there are no scatterers in the bulk and that the electron wavefunction vanishes at the boundary of semi-infinite lattice [5, 2].

A second, in a sense closely related, motivation for the paper stems from the scattering of the two-dimensional electron gas off step edges and point defects [104, 75, 66, 10, 86]. The electronic structure, which is 'homogeneous' on a perfect surface [62, 103] is, thus, perturbed by the presence of point defects or line defects such as step edges or dislocations [96]. It is known that this phenomenon, for example that observed in Cu(111) [20], leads to spatial oscilla-

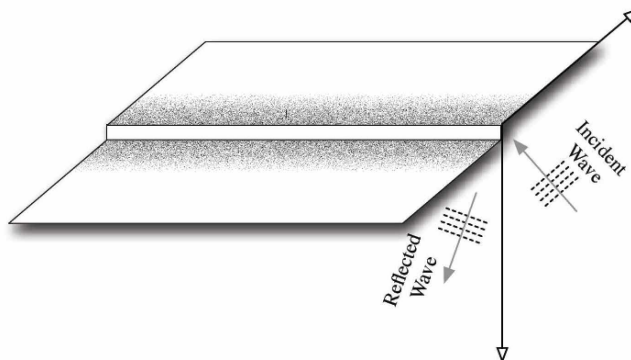


Figure 1: Semi-infinite half space with step. Incident bulk (conduction) electron schematically shown.

tions (or quantum-mechanical interference patterns); the influence of bulk band states in such standing wave patterns observed in STM has been also demonstrated [92, 56]. For instance, in Fig. 2 of [92] a few oscillations are attributed to the scattering of bulk states at monatomic step which disperse as the energy is increased. In the same vein, the energy dependence of the contribution of bulk state electrons to the electron standing-wave patterns at the Au (111) surface have been also systematically investigated [105]. Patterns have been observed that originate from the scattering of bulk electrons between subsurface impurities as well as those on the surface [128, 90]. Thus, electron interference can be induced by electron scattering at surface defects [58], step edges, adsorbates, etc, that cause scattering patterns in the form of standing waves. In addition to the surface states [20, 43, 100] or the image-potential states [138], the bulk states are also held responsible for some of the observed standing waves [94, 92, 105]. The presented work concerns the bulk electron scattering from edges, ignoring the role of localized edge states, and focussing on the essential role of the dependence on incoming angle and energy of electrons [24] (see Fig. 3 for bands).

With above backdrop, in this paper the scattering of electronic waves in square and triangular lattice half-planes by a surface step has been analyzed using the nearest-neighbour *tight binding approximation* (with a schematic illustration in Fig. 2). Electronic states of crystalline systems with surfaces, specially at low temperatures, have been also sought earlier using the tight-binding approximation [57]¹; see its rich history as revealed by the analyses of

¹In chemistry this is known as the LCAO representation (linear combination of atomic orbitals), in physics it is usually called the tight-binding representation [120]. The present model is the nearest neighbor tight-binding approximation [17] as called by physicists and among chemists it is related to what is known as the Hückel approximation [48]. The electronic band structure is calculated using an approximate set of wavefunctions based upon superposition of orbitals located at each individual atomic site [95]. The tight-binding approximation [57] is typically characterized by two terms: a kinetic term that describes the hopping of particles

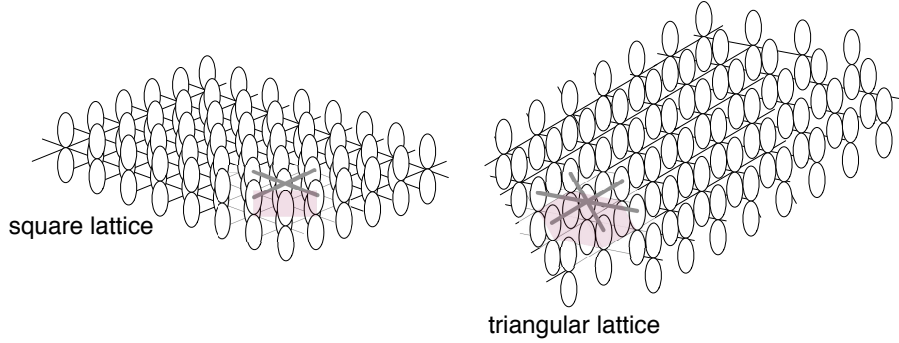


Figure 2: Schematic of square and triangular lattice structures with p -like orbital per atom and one atom per unit cell.

[34, 35, 36, 37], as well as its extensions [4, 63, 65, 19, 22, 129]. An elaborate and classical discussion on several types of surfaces, interfaces, overlayer systems, super-lattices, defects at surfaces or interfaces, etc., is provided by [97] within the context of the tight binding and the scattering theoretical approach for locally perturbed solids [61, 120]. The present paper, however, employs an exceedingly simple formulation in comparison though the calculations are less intensive and analysis is tractable. For the case of infinite square and triangular lattices with a finite [111, 113] or a semi-infinite [108, 112] slit, while assuming the vanishing of the electronic wavefunction at the ‘missing’ sites, the associated scattering problems have been recently analyzed by [108, 111, 112, 113] using the same method [84] as that implemented in the present paper.

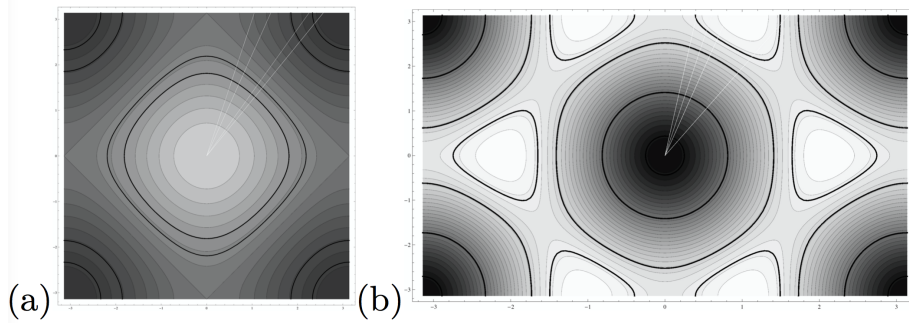


Figure 3: Energy bands $\mathcal{E}_\kappa(\kappa_x, \kappa_y)$ in the bulk for (a) $\mathfrak{S}_{\bullet\bullet}$ and (b) $\mathfrak{T}_{\bullet\bullet}$.

between neighboring sites in the potential and an on-site interaction term (assumed to be zero as it appears as an offset only).

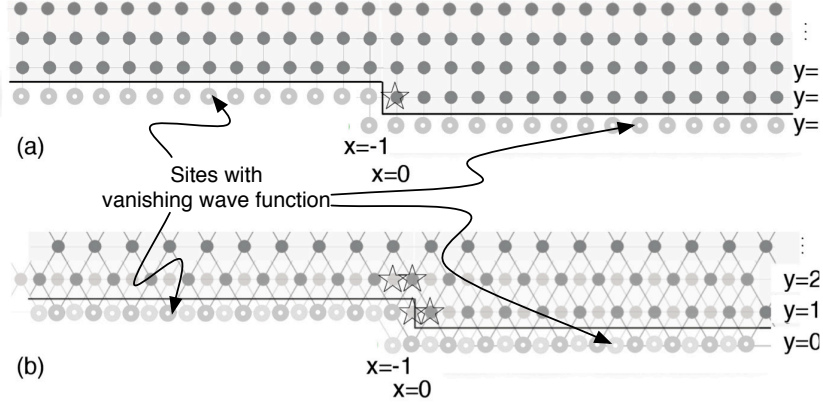


Figure 4: Semi-infinite square and triangular lattice structure with step (a) $\mathfrak{S}_{\bullet\bullet}$, (b) $\mathfrak{T}_{\bullet\bullet}$.

1 Square lattice model

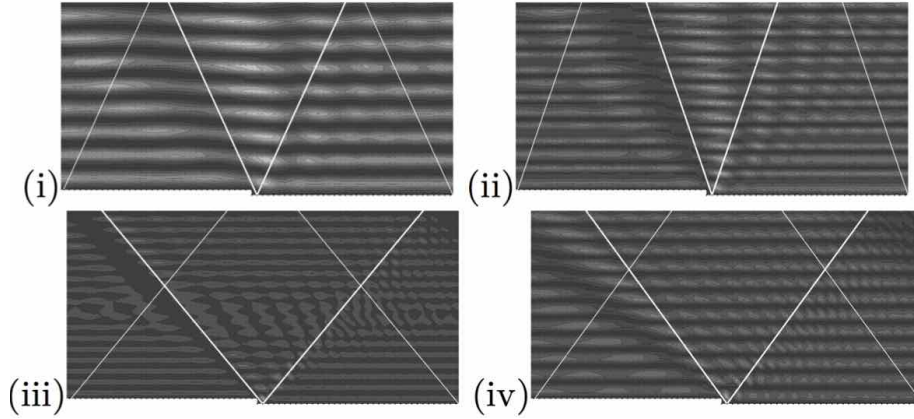


Figure 5: $|\psi|^2$ for $\mathfrak{S}_{\bullet\bullet}$. (i) $\beta^{-1}\mathcal{E}_\kappa = -3.38$, $\kappa^{\text{inc}} = 0.81$, $\Theta = 65.8$ deg, (ii) $\beta^{-1}\mathcal{E}_\kappa = -2.56$, $\kappa^{\text{inc}} = 1.27$, $\Theta = 71.5$ deg, (iii) $\beta^{-1}\mathcal{E}_\kappa = 0.84$, $\kappa^{\text{inc}} = 2.8$, $\Theta = 50.7$ deg, and (iv) $\beta^{-1}\mathcal{E}_\kappa = 1.52$, $\kappa^{\text{inc}} = 2.57$, $\Theta = 54.33$ deg. $A = 1$, $\mathcal{E}_2 = 10^{-3}$, $N_{\text{grid}} = 71$, $N_{\text{pml}} = 58$.

Let a semi-infinite two-dimensional square lattice with a surface step be

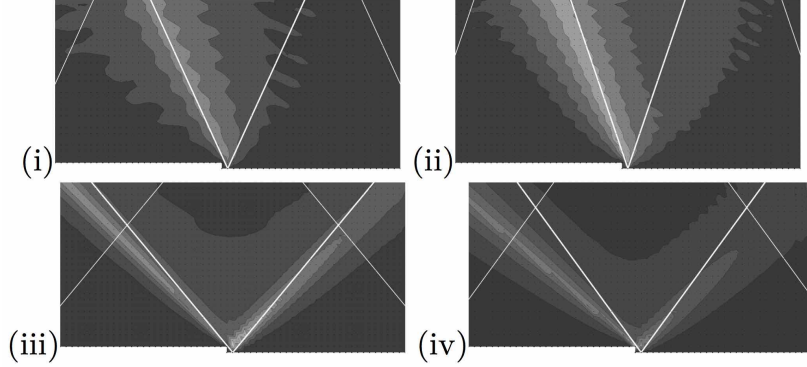


Figure 6: $|\psi - \psi^g|$ for $\mathfrak{S}_{\bullet\bullet}$. The details correspond to Fig. 5.

denoted by $\mathfrak{S}_{\bullet\bullet}$, i.e.,

$$\mathfrak{S}_{\bullet\bullet} := \{m\hat{\mathbf{i}} + n\hat{\mathbf{j}} | m \in \mathbb{Z}, n \in \mathbb{Z}^+ \setminus \{0, 1\}\} \cup \{m\hat{\mathbf{i}} + \hat{\mathbf{j}} | m \in \mathbb{Z}^+\}, \quad (1.1)$$

where $\hat{\mathbf{i}}$ and $\hat{\mathbf{j}}$ form the standard basis of two dimensional space \mathbb{R}^2 . The geometric structure of step in semi-infinite square lattice is schematically illustrated in Fig. 4(a).

An electronic model based on the tight-binding approximation is considered, where the tunneling amplitude for an electron to hop from one atom to the next is determined by the coupling matrix element β (i.e., the transfer integral between nearest-neighbor sites). For the two-dimensional square lattice with either one s -like orbital or one p -like orbital per atom and one atom per unit cell, the tight-binding Hamiltonian can be explicitly written (within the second quantization) in the following form²

$$\mathcal{H} = -\beta \sum_{\mathbf{x} \in \mathbb{Z}, \mathbf{y} \in \mathbb{Z}^+} (a_{\mathbf{x}+1, \mathbf{y}}^\dagger a_{\mathbf{x}, \mathbf{y}} + a_{\mathbf{x}, \mathbf{y}+1}^\dagger a_{\mathbf{x}, \mathbf{y}} + h.c.), \quad (1.2)$$

where $a_{\mathbf{x}, \mathbf{y}}^\dagger$ and $a_{\mathbf{x}, \mathbf{y}}$ are the *creation* and *annihilation* operators on the lattice site (\mathbf{x}, \mathbf{y}) respectively. In this context, the bulk band structure of two-dimensional square lattice with one atom per unit cell [50] is easily found to be given by

$$\mathcal{E}_\kappa = \mathcal{E}(\kappa_x, \kappa_y) := -\beta(2 \cos \kappa_x + 2 \cos \kappa_y), \quad (1.3)$$

$$\kappa_x \in [-\pi, \pi], \kappa_y \in [0, \pi].$$

Applying the quantum mechanical bra-ket notation, and the Fourier transform (A.1) along x -axis, the electronic wavefunction is expressed as $|\Psi(\xi)\rangle =$

²The perturbation in lattice spacing or β near the boundary is ignored in this simple model. In (1.2), using the traditional symbolic choice, h.c. stands for the phrase ‘Hermitian conjugate’ [131].

$\sum_{\mathbf{y} \in \mathbb{Z}^+} \psi_{\mathbf{y}}(\xi) \alpha_{\xi}^{\dagger}(\mathbf{y}) |0\rangle$, where α_{ξ} (resp. α_{ξ}^{\dagger}) denote the Fourier transform of $a_{\mathbf{x}}$, (resp. $a_{\mathbf{x},\cdot}^{\dagger}$), and $|0\rangle$ denotes the vacuum wavefunction (as a reference). Then, the Schrödinger equation $\mathcal{H}(\xi)|\Psi(\xi)\rangle = \mathcal{E}_{\kappa}|\Psi(\xi)\rangle$, leads to the difference equation

$$\beta^{-1} \mathcal{E}_{\kappa} \psi_{\mathbf{y}} = -\psi_{\mathbf{y}+1}(\xi) - \psi_{\mathbf{y}-1}(\xi) - 2 \cos \xi \psi_{\mathbf{y}}(\xi). \quad (1.4)$$

The boundary condition for $\mathfrak{S}_{\bullet\bullet}$ is $\psi_{\mathbf{y};+}(\xi)|_{\mathbf{y}=0} = \psi_{\mathbf{y};-}(\xi)|_{\mathbf{y}=1} = 0$ using the notation of (A.1).

Suppose ψ^{inc} describes the *incident electronic wave*. It is assumed that ψ^{inc} is given by

$$\psi_{\mathbf{x},\mathbf{y}}^{\text{inc}} := A e^{-i\kappa_x \mathbf{x} - i\kappa_y \mathbf{y}}, \quad (\mathbf{x}, \mathbf{y}) \in \mathbb{Z}^2, \quad (1.5)$$

where $A \in \mathbb{C}$ is constant. As stated above, the corresponding energy is $\mathcal{E}_{\kappa} = \mathcal{E}(\kappa_x, \kappa_y)$. The total wavefunction ψ at an arbitrary site in $\mathfrak{S}_{\bullet\bullet}$ is a sum of the incident wavefunction ψ^{inc} and the scattered wavefunction ψ^s . With $\psi_{\cdot,\mathbf{y}}$ as the inverse Fourier transform of $\psi_{\mathbf{y}}(\cdot)$, the equation satisfied by the (discrete) wavefunction ψ on $\mathfrak{S}_{\bullet\bullet}$ is

$$\psi_{\mathbf{x}+1,\mathbf{y}} + \psi_{\mathbf{x}-1,\mathbf{y}} + \psi_{\mathbf{x},\mathbf{y}+1} + \psi_{\mathbf{x},\mathbf{y}-1} + \beta^{-1} \mathcal{E}_{\kappa} \psi_{\mathbf{x},\mathbf{y}} = 0, \quad \mathbf{x} \in \mathbb{Z}, \mathbf{y} > 1 \text{ or } \mathbf{x} \in \mathbb{Z}^+, \mathbf{y} = 1, \quad (1.6a)$$

$$\text{and } \psi_{\mathbf{x},0} = 0, \mathbf{x} \in \mathbb{Z}^+, \psi_{\mathbf{x},1} = 0, \mathbf{x} \in \mathbb{Z}^-. \quad (1.6b)$$

The wavefunction based on the numerical solution of the problem, i.e., (1.6a), (1.6b) with (1.5), is illustrated in Fig. 5. The difference between the total wavefunction and the geometric wavefield (associated with specular reflection as described in Appendix C) is illustrated in Fig. 6. Following the tradition [25], it is assumed that $\mathcal{E}_{\kappa} \simeq \mathcal{E}_{\kappa} + i0$, with $\beta^{-1} \mathcal{E}_{\kappa} \in [-4, 4] \setminus \{0, \pm 4\}$ [106]. Due to the absence of localized (surface) waves on the assumed structure of semi-infinite square lattice model [97] (see also [115] and Appendix C of [114] where the connection with one dimensional models of [70, 139] becomes clear), there is no loss of generality in the choice of the incident wave parameters.

Notice that the sites at $\mathbf{x} \geq 0, \mathbf{y} = 0$ as well as $\mathbf{x} < 0, \mathbf{y} = 1$ are assigned zero wavefunction (1.6b), as also shown in Fig. 4(a) as empty dots. Based on the manipulations and constructions documented in [121] and [107, 108] (see also Appendix A for a brief recollection), as well as several similar and related techniques applied by researchers few decades ago (for instance, [73, 32]), the scattered wavefunction in the lattice half-plane (1.1) is found to be given by

$$\psi_{\mathbf{y}}^{sF} = \psi_1^{sF} \lambda^{\mathbf{y}-1} \quad (1.7)$$

using the definition of λ stated in (A.2c) and the general solution (A.3). As an analogue of (1.6a) for $\mathbf{y} = 1$, $(-4 - \beta^{-1} \mathcal{E}_{\kappa}) \psi_{\mathbf{x},1} = (\psi_{\mathbf{x}-1,1} + \psi_{\mathbf{x}+1,1} + \psi_{\mathbf{x},2} + \psi_{\mathbf{x},0} - 4\psi_{\mathbf{x},1}) H(\mathbf{x})$, so that

$$\begin{aligned} & (-4 - \beta^{-1} \mathcal{E}_{\kappa}) \psi_{1;-}^s + (-4 - \beta^{-1} \mathcal{E}_{\kappa}) \psi_{1;-}^{\text{inc}} \\ & = \psi_{-1,1}^s - z \psi_{0,1}^s + (z + z^{-1} + \beta^{-1} \mathcal{E}_{\kappa}) \psi_{1;+}^s + \psi_{2;+}^s - \psi_{0;+}^{\text{inc}}. \end{aligned} \quad (1.8)$$

Due to their frequent appearance in the rest of the paper, it is convenient to introduce the definitions

$$\begin{aligned} z_P := e^{-i\kappa x} \in \mathbb{C}, \delta_{D^+}(z) &:= \sum_{n=0}^{+\infty} z^{-n}, z \in \mathbb{C} \\ \delta_{D^-}(z) &:= \sum_{n=-\infty}^{-1} z^{-n}, z \in \mathbb{C}. \end{aligned} \quad (1.9)$$

In context of the well-posedness of the Wiener–Hopf problem [116] (as described in its §2), consider the introduction of a factor $e^{-\epsilon|x|}$ in ψ^{inc} ; with an implicit assumption of the limit $\epsilon \rightarrow 0^+$. Using (1.8) and (1.6b), as well as the expression ψ^{inc} (1.5) and Q (A.2b), it is found that

$$w - \psi_{0,+}^{\text{inc}} + Q\psi_{1,-}^s = Q\psi_1^{sF} - \psi_{2,+}^s, \quad (1.10a)$$

$$\psi_{1,-}^s(z) = -Ae^{-i\kappa y} \delta_{D^-}(zz_P^{-1}e^{-\epsilon}), \quad (1.10b)$$

$$\text{where } w(z) := \psi_{-1,1}^s - z\psi_{0,1}^s. \quad (1.10c)$$

After the substitution of (1.7), i.e., the expression of ψ_2^{sF} in terms of ψ_1^{sF} as $\psi_2^{sF} = \psi_1^{sF}\lambda$, a rearrangement of (1.10a) and the definition of the one-sided discrete Fourier transform (A.1) leads to the Wiener–Hopf equation for ψ_2^{sF} (i.e., $\psi_{2,+}^s$ and $\psi_{2,-}^s$) as

$$\begin{aligned} \mathcal{L}\psi_{2,+}^s(z) + \psi_{2,-}^s(z) &= (1 - \mathcal{L}(z))(w(z)) \\ -AQe^{-i\kappa y} \delta_{D^-}(zz_P^{-1}e^{-\epsilon}) - A\delta_{D^+}(zz_P^{-1}e^{+\epsilon}), \end{aligned} \quad (1.11a)$$

$$\text{where } \mathcal{L} = \frac{1}{2}\left(1 + \frac{r\hat{h}}{Q}\right), \text{ on } \mathcal{A}. \quad (1.11b)$$

The symbol \mathcal{A} stands for an annulus in the complex plane where the Wiener–Hopf formulation [84] is well-posed; see §2 of [116] for the relevant mathematical analysis. This concludes the mathematical formulation of the case of square lattice half-plane with step (according to the schematic depiction of Fig. 4(a)).

2 Triangular lattice model

Let

$$\begin{aligned} \mathfrak{T}_{\bullet\bullet} := \{m\mathbf{e}_1 + n\mathbf{e}_2, m \in \mathbb{Z}, n \in \mathbb{Z}^+ \setminus \{0, 1\}\} \\ \cup \{m\mathbf{e}_1 + \mathbf{e}_2, m \in \mathbb{Z}^+\}, \end{aligned} \quad (2.1)$$

$$\text{with } \mathbf{e}_1 = b\hat{\mathbf{i}}, \mathbf{e}_2 = \frac{1}{2}b\hat{\mathbf{i}} + \frac{\sqrt{3}}{2}b\hat{\mathbf{j}},$$

represent the semi-infinite triangular lattice half-plane, as also shown schematically in Fig. 4(b). Due to the presence of slant bonds in the triangular lattice, the formulation is placed in the sense of a union with a replicated lattice $\mathfrak{T}_{\bullet\bullet}^{\text{R}}$ (same as the construction introduced by [112]). This allows a rectangular coordinate system to be used in place of the usual ‘slant’ coordinates for triangular

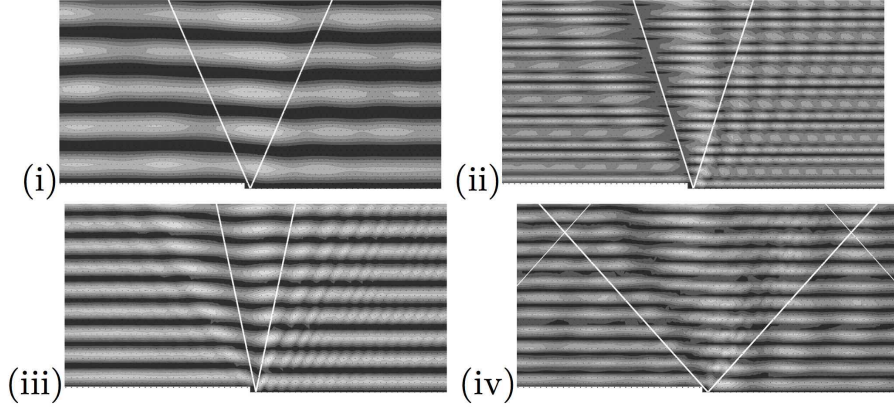


Figure 7: $|\psi|^2$ for $\mathfrak{T}_{\bullet\bullet}$. (i) $\beta^{-1}\mathcal{E}_\kappa = -2.75, \kappa^{\text{inc}} = 0.5, \Theta = 65.8$ deg, (ii) $\beta^{-1}\mathcal{E}_\kappa = -0.75, \kappa^{\text{inc}} = 1.63, \Theta = 72.6$ deg, (iii) $\beta^{-1}\mathcal{E}_\kappa = 1.84, \kappa^{\text{inc}} = 2.88, \Theta = 78.3$ deg, and (iv) $\beta^{-1}\mathcal{E}_\kappa = 2.52, \kappa^{\text{inc}} = 3.4, \Theta = 48.5$ deg. $A = 1, \mathcal{E}_2 = 10^{-3}, N_{\text{grid}} = 101, N_{\text{pmt}} = 82$.

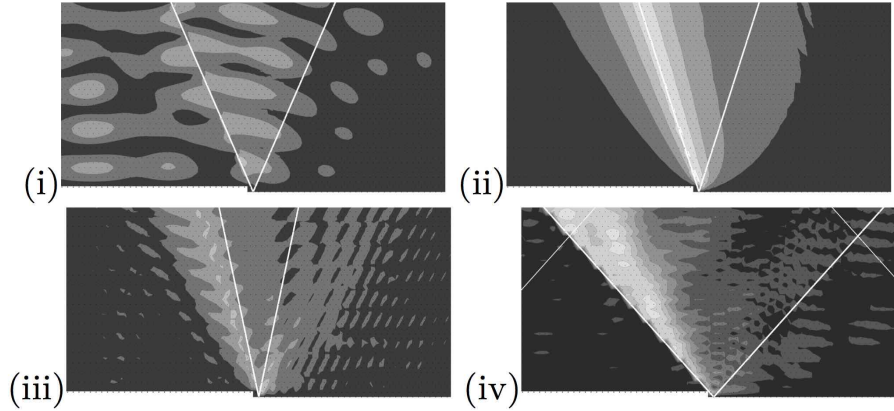


Figure 8: $|\psi - \psi^g|$ for $\mathfrak{T}_{\bullet\bullet}$. The details correspond to Fig. 7.

structure. The union of both lattices is a rectangular lattice, denoted by \mathfrak{R} , with a period $b/2$ horizontally and $\sqrt{3}b/2$ vertically. The wavefunction at a site in \mathfrak{R} , indexed by its *lattice coordinates* $(\mathbf{x}, \mathbf{y}) \in \mathbb{Z}^2$, is denoted by $\psi_{\mathbf{x}, \mathbf{y}}^s \in \mathbb{C}$. It is assumed that each site in \mathfrak{R} is connected (atmost) with its six nearest neighbors (as part of $\mathfrak{T}_{\bullet\bullet}$ or $\mathfrak{T}_{\bullet\bullet}^{\text{R}}$).

Drawing benefit from the rectangular lattice coordinates (so that there is a symbolic similarity with the square lattice formulation presented in the previous section), it is assumed that the incident electronic wavefunction ψ^{inc} is given by an expression of the form (1.5), where $A \in \mathbb{C}$ is constant. The discussion

concerning the tight-binding approximation follows that provided above in §1. Using the expression of the incident wave (1.5), note that the energy band relation $\mathcal{E}_\kappa = \mathcal{E}(\kappa_x, \kappa_y)$ for the triangular lattice satisfies [14, 47]

$$\begin{aligned} \frac{3}{2}(3 + \beta^{-1}\mathcal{E}_\kappa) - 6 + 2 \cos 2\kappa_x + 4 \cos \kappa_x \cos \kappa_y &= 0, \\ \kappa_x \in [-\pi, \pi], \kappa_y \in [0, \pi]. \end{aligned} \quad (2.2)$$

Because $\mathfrak{T}_{\bullet\bullet}$ and $\mathfrak{T}_{\bullet\bullet}^R$ are ‘uncoupled’, $[-\pi, \pi]^2$ is *not* the fundamental domain for $\mathfrak{T}_{\bullet\bullet}$ [14]; rather a hexagon shaped polygonal region, denoted by BZ_1 and also known as the first Brillouin zone [14], is the fundamental domain. Henceforth, it is assumed that $(\kappa_x, \kappa_y) \in \text{BZ}_1 \subset [-\pi, \pi]^2$. The lattice wave number and the angle of incidence of ψ^{inc} are defined by the relations $\kappa_x = \frac{1}{2}\kappa \cos \Theta$, $\kappa_y = \frac{\sqrt{3}}{2}\kappa \sin \Theta$, with $\kappa = \kappa_1 + i\kappa_2$, $\kappa_1 \geq 0$. In addition to the pass band of the bulk lattice, there does not exist a surface wave on the semi-infinite triangular lattice with a Dirichlet boundary [115, 97], hence there is no loss of generality in the choice (1.5) of incident wave.

The total wavefunction ψ , a sum of the incident wavefunction ψ^{inc} and the scattered wavefunction ψ^s , of an arbitrary site in the lattice \mathfrak{R} (and, therefore, in triangular lattice $\mathfrak{T}_{\bullet\bullet}$ or $\mathfrak{T}_{\bullet\bullet}^R$) satisfies the discrete Helmholtz equation (as a counterpart of (1.6a))

$$\begin{aligned} \psi_{x+1,y+1} + \psi_{x+1,y-1} + \psi_{x-1,y+1} + \psi_{x-1,y-1} \\ + \psi_{x+2,y} + \psi_{x-2,y} + \frac{3}{2}(\beta^{-1}\mathcal{E}_\kappa - 1)\psi_{x,y} &= 0, \\ \mathbf{x} \in \mathbb{Z}, \mathbf{y} > 1 \text{ or } \mathbf{x} \in \mathbb{Z}^+, \mathbf{y} = 1, \end{aligned} \quad (2.3)$$

along with the vanishing wavefunction condition (1.6b). The total electronic wavefunction based on the numerical solution of above problem is illustrated in Fig. 7 while the difference between the total wavefunction and the geometric wavefield (associated with specular reflection as described in Appendix C) is illustrated in Fig. 8.

The solution of the discrete Helmholtz equation (2.3) (see Fig. 4(b)), is (1.7), where ψ_1^{sF} is unknown function modulo its ‘half’ portion on the step discontinuity and λ given by (A.2c) using the definition of Q provided in (A.4). Using (1.7) and the form of ψ^{inc} (1.5), as well as (2.3) for $\mathbf{y} = 1, \mathbf{x} \geq 0$ after application of the discrete Fourier transform, and the data $\psi_{x,y} = 0$ for $\mathbf{y} = 1, \mathbf{x} \in \mathbb{Z}^-$ and $\mathbf{y} = 0, \mathbf{x} \in \mathbb{Z}^+$, it follows that (analogous to (1.10))

$$\begin{aligned} (z + z^{-1})Q(z)\psi_{1,+}^s(z) &= w(z) + w^{\text{inc}}(z) \\ &\quad + (z + z^{-1})\psi_{2,+}^s(z), \end{aligned} \quad (2.4a)$$

$$\psi_{1,-}^s(z) = -Ae^{-i\kappa_y} \delta_{D-}(zz^{-1}), \quad (2.4b)$$

where the complex functions w and w^{inc} are

$$\begin{aligned} w(z) &:= -z^2 \psi_{0,1}^s + z(-\psi_{1,1}^s - \psi_{0,2}^s) \\ &\quad + (-Ae^{-i\kappa_y} z_P^{-2} + \psi_{-1,2}^s) - Ae^{-i\kappa_y} z_P^{-1} z^{-1}, \\ w^{\text{inc}}(z) &= z \psi_{0,0}^{\text{inc}} - \psi_{-1,0}^{\text{inc}}. \end{aligned} \quad (2.4c)$$

By virtue of the expression (1.7), it follows that $\psi_2^{sF} = \psi_1^{sF} \lambda$ holds; further, upon substitution of the same in the equation (2.4a), after simplification, the discrete Wiener–Hopf equation for $\psi_{2,+}^s$ and $\psi_{2,-}^s$ is found to be (contrast with (1.11a))

$$\begin{aligned} \mathcal{L}(z) \psi_{2,+}^s(z) + \psi_{2,-}^s(z) &= (1 - \mathcal{L}(z)) \left(\frac{w(z) + w^{\text{inc}}(z)}{z + z^{-1}} \right) \\ &\quad - QAe^{-i\kappa_y} \delta_{D-}(zz_P^{-1} e^{-\epsilon}) - A\delta_{D+}(zz_P^{-1} e^{+\epsilon}), \quad \forall z \in \mathcal{A}, \end{aligned} \quad (2.5)$$

where \mathcal{L} is given by (1.11b). Again, \mathcal{A} is an annulus in the complex plane suitable for the Wiener–Hopf formulation [84] (analogous to that for the case of square lattice). This completes the problem formulation for the triangular lattice half-plane with step as illustrated in Fig. 4(b).

3 The exact solution

After a standard application of the Wiener–Hopf technique (detailed calculations are presented in Appendix D.1 for $\mathfrak{S}_{\bullet\bullet}$ and in Appendix D.2 for $\mathfrak{T}_{\bullet\bullet}$) for solving both equations (1.11a) and (2.5), it is found that the function ψ_1^{sF} can be expressed as

$$\begin{aligned} \psi_1^{sF}(z) &= Az \mathcal{K}(z) \left(\frac{\mathbf{C}_{0B}}{z - z_P \alpha_B} + \frac{\mathbf{C}_{0A}}{z - z_P \alpha_A} \right), \\ \alpha_{A,B} &= e^{\mp \epsilon}, \\ \mathcal{K}(z) &:= \frac{1}{(1 - z_q^{1+\tau} z^{-1-\tau}) \mathcal{L}_+(z)}, \\ \mathbf{C}_{0B} &:= e^{-i\kappa_y} (1 - z_q^{1+\tau} z_P^{-1-\tau}) \mathcal{L}_+(z_P), \\ \mathbf{C}_{0A} &:= - (z_P + z_P^{-1})^\tau \frac{\mathcal{L}_-^{-1}(z_P)}{z_q^{-1-\tau} - z_P^{1+\tau}}, \end{aligned} \quad (3.1)$$

for $z \in \mathcal{A}$ where the choice $\tau = 0$ leads to the expression for $\mathfrak{S}_{\bullet\bullet}$ while $\tau = 1$ corresponds to $\mathfrak{T}_{\bullet\bullet}$.

Combining (3.1) with (1.7), $\psi_{x,y}^s$ is eventually determined by the inverse discrete Fourier transform,

$$\psi_{x,y}^s = \frac{1}{2\pi i} \oint_{\mathcal{C}} \psi_y^{sF}(z) z^{x-1} dz, \quad (3.2)$$

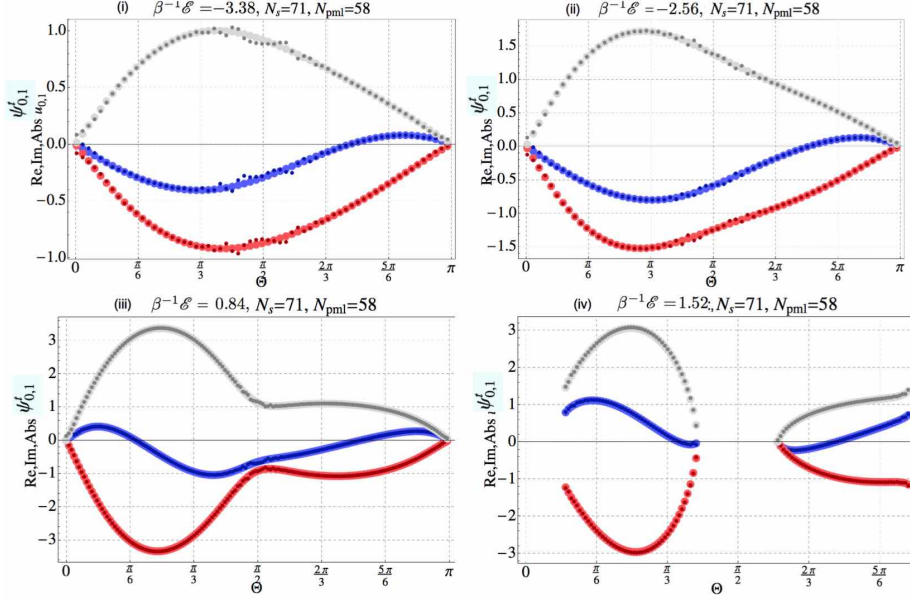


Figure 9: $\text{Re } \psi_{0,1}$ (blue), $\text{Im } \psi_{0,1}$ (red), and $|\psi_{0,1}|$ (black) vs $\Theta \in (0, \pi)$ for four choices of $\beta^{-1}\mathcal{E}_\kappa =$ (i) -3.38 , (ii) -2.56 , (iii) 0.84 , (iv) 1.52 . $N_{\text{grid}} = 71$, $N_{\text{pml}} = 58$ for $\mathfrak{S}_{\bullet\bullet}$.

where \mathcal{C} is a rectifiable, closed, counterclockwise contour in the annulus \mathcal{A} . These expressions can be simplified further in a manner akin to the results presented recently by [110, 111]. For example in case of $\mathfrak{S}_{\bullet\bullet}$, using (D.2) and (1.10a), the expression for $\psi_{1,+}^s$ can be found and $\psi_{0,1}$ (consequently w by (1.10c)) is obtained as

$$\psi_{0,1} = A l_{+0}^{-1} (\mathcal{C}_{0B} + \mathcal{C}_{0A}). \quad (3.3)$$

In fact, as a rather curious observation, it is also found that in case of $\mathfrak{T}_{\bullet\bullet}$ (as detailed in Appendix D.2 in order to arrive at (D.6b)), the same expression holds for $\psi_{0,1}$ (which, incidentally, equals $\psi_{1,1}$ modulo a factor $e^{-i\kappa x}$). For convenience, the corresponding sites $(0,1)$ in $\mathfrak{S}_{\bullet\bullet}$ and $(1,1)$ in $\mathfrak{T}_{\bullet\bullet}$ are marked by a star in Fig. 4(a) and Fig. 4(b), respectively. The graphical results are provided in Fig. 9 for $\psi_{0,1}$ in $\mathfrak{S}_{\bullet\bullet}$ and in Fig. 10 for $\psi_{1,1}$ in $\mathfrak{T}_{\bullet\bullet}$, for various choices of incident electronic energy \mathcal{E}_κ versus the angle of incidence Θ ; Fig. 11 presents the same for various choices of the angle of incidence Θ versus the incident electronic energy \mathcal{E}_κ . The darker dots correspond to numerical solution depicted in Fig. 5 and Fig. 7.

Employing (3.2), above description provides the complete solution of the wave propagation problem in integral form. Notice that the ‘form’ of the solution (3.2) has been intentionally chosen to be the same as its counterpart for the discrete Sommerfeld problems, which were recently introduced and analyzed by

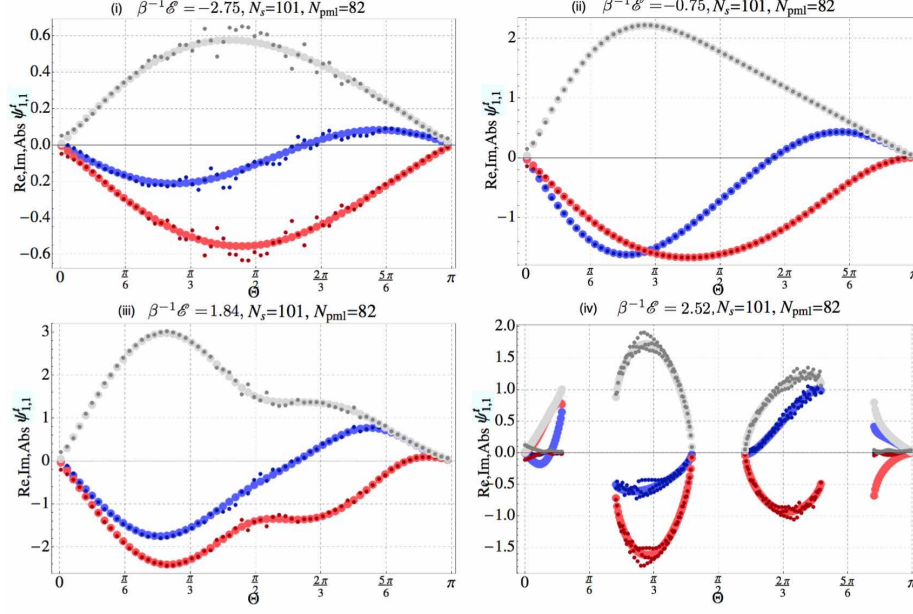


Figure 10: $\text{Re } \psi_{1,1}$ (blue), $\text{Im } \psi_{1,1}$ (red), and $|\psi_{1,1}|$ (black) vs $\Theta \in (0, \pi)$ for four choices of $\beta^{-1}\mathcal{E}_\kappa =$ (i) -2.75 , (ii) -0.75 , (iii) 1.84 , (iv) 2.52 . $N_{\text{grid}} = 101$, $N_{\text{pml}} = 82$ for $\mathfrak{I}_{\bullet\bullet}$.

the author [107, 108, 112]. The benefit of this choice appears below, in the form of direct application of the detailed asymptotic analysis of the scattered wavefunction in far-field [107, 112] (see also [116]).

4 Far Field Approximation

For

$$\beta^{-1}\mathcal{E}_\kappa \in \begin{cases} (-4, 0) \cup (0, 4) & \text{for } \mathfrak{S}_{\bullet\bullet} \\ (-3, 7/3) \cup (7/3, 3) & \text{for } \mathfrak{I}_{\bullet\bullet} \end{cases}, \quad (4.1)$$

(recall that $\mathcal{E}_\kappa \simeq \mathcal{E}_\kappa + i0$, $\kappa \simeq \kappa_1 + i0$) the analysis of asymptotic approximation [12, 27, 29] of the scattered wavefunction in far-field follows after a suitable modification of the expressions stated by [107] and [112], respectively. For example, \mathcal{X} and \mathcal{C}_0 from (3.1) are used in place of the definitions provided by [107, 112] (note that the corresponding \mathcal{L} is given by (1.11b), which does not admit explicit factors as found in case of [107]). It is found that a far-field asymptotic approximation for ψ^s is

$$\psi_{x,y}^s \sim \sum_S \psi_{x,y}^s|_S + \sum_{s=A,B} \psi_{x,y}^s|_{Ps}, \quad (4.2a)$$

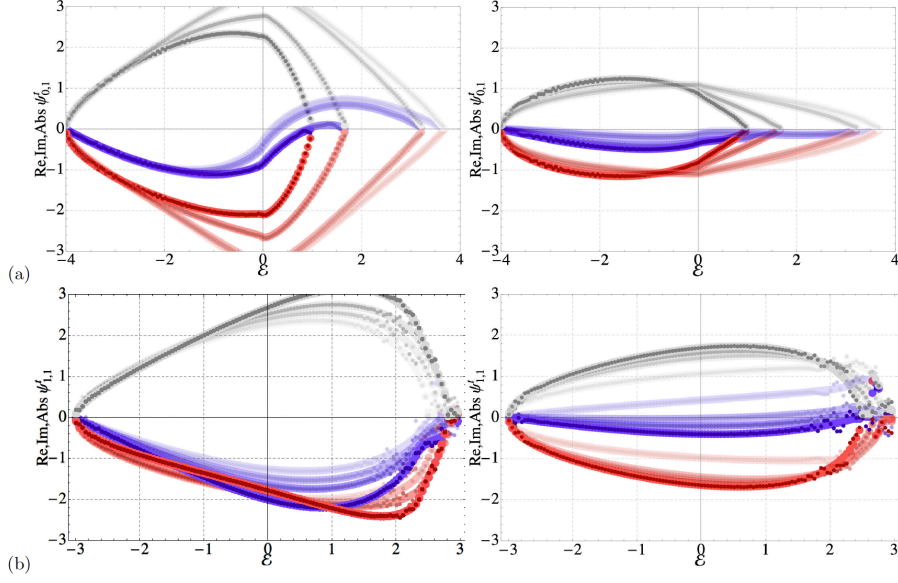


Figure 11: (a) $\text{Re } \psi_{0,1}$ (blue), $\text{Im } \psi_{0,1}$ (red), and $|\psi_{0,1}|$ (black) vs $\beta^{-1}\mathcal{E}_\kappa \in (-4, 4)$ for (left) given Θ (right) Θ on $\mathfrak{S}_{0,1}$. The darker shades correspond to larger $\Theta \in \{71.52, 65.79, 54.33, 50.73\}$ (deg) on left and correspond to smaller $\Theta \in \{108.48, 114.21, 125.67, 129.27\}$ on right. (b) $\text{Re } \psi_{1,1}$ (blue), $\text{Im } \psi_{1,1}$ (red), and $|\psi_{1,1}|$ (black) vs $\beta^{-1}\mathcal{E}_\kappa \in (-3, 3)$ for (left) given Θ (right) Θ on $\mathfrak{S}_{1,1}$. The darker shades correspond to smaller $\Theta \in \{78.33, 72.61, 66.88, 48.54\}$ (deg) on left and $\Theta \in \{101.67, 107.39, 113.12, 131.46\}$ (deg) on right. For (a) $N_{\text{grid}} = 71, N_{\text{pml}} = 58$, while for (b) $N_{\text{grid}} = 101, N_{\text{pml}} = 82$.

where

$$\psi_{x,y}^s|_S \sim -A \frac{(1 + i \text{sgn}(\eta''(\xi_S))) \mathcal{X}(z_S) e^{iR\Phi(\xi_S)}}{2\sqrt{\pi} \left(\frac{2}{\sqrt{3}} \right)^\tau R |\eta''(\xi_S)| \sin \theta)^{\frac{1}{2}}} \left(\sum_{s=A,B} \frac{C_{0s}}{\alpha_s z_P z_S^{-1} - 1} \right) e^{-i\eta(\xi_S)}, \quad (4.2b)$$

and³

$$\psi_{x,y}^s|_{PB} = \psi_{x,y}^{rB} H(\theta - \theta_r), \psi_{x,y}^s|_{PA} = -\psi_{x,y}^{rA} H(\theta_r - \theta), \quad (4.2c)$$

with η and ϕ defined in (E.3) and (E.5), R and θ defined in (E.1) and (E.4), and $\mathcal{X}, C_{0A}, C_{0B}$ given in (3.1) while the saddle point z_S ($z_S = e^{-i\xi_S}$) is described in [107, 112] (also discussed briefly in Appendix E). Recall that $\tau = 0$ for $\mathfrak{S}_{0,1}$.

³The expression for $\psi_{x,y}^s|_{Ps}$, the residue contribution of the pole at z_P is obtained after several manipulations which are omitted.

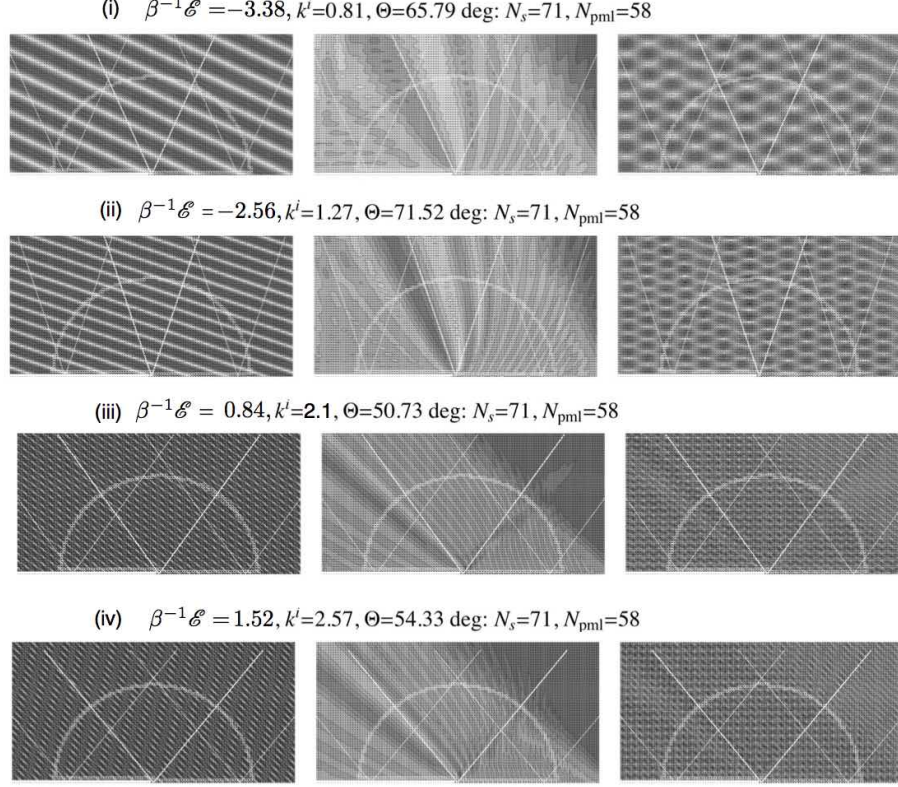


Figure 12: Incident $\Re\psi^{\text{inc}}$ (left), scattered $|\psi^s|$ (center), and $\Re\psi$ (right) wavefunction for the semi-infinite square lattice structure with step $\mathfrak{S}_{\bullet\bullet}$. The details correspond to Fig. 5.

while $\tau = 1$ for $\mathfrak{T}_{\bullet\bullet}$. For the case of $\mathfrak{S}_{\bullet\bullet}$, there is only one saddle point and θ_r is defined such that for $\xi_S = \kappa_x$ when $\theta = \theta_r$. For the case of $\mathfrak{T}_{\bullet\bullet}$, the notation \sum_S denotes the sum over all saddle points of the diffraction integral that are located inside the fundamental domain of \mathfrak{R} above, and θ_r is defined such that for $\theta = \theta_r$, $\xi_S = \kappa_x$ for $\beta^{-1}\mathcal{E}_\kappa \in (-3, 7/3)$, while $\xi_{S;l} = \kappa_x$ or $\xi_{S;r} = \kappa_x$ for $\beta^{-1}\mathcal{E}_\kappa \in (7/3, 3)$. For more details concerning the saddle point analysis for the relevant diffraction integral for triangular lattice structure, see [112].

5 Numerical Results

Since the equations (2.3), and other equations corresponding to the defect, are algebraic, the numerical solution on a $(2N_{\text{grid}} + 1) \times N_{\text{grid}}$ square grid Ω (mapped to its appropriate counterpart in case of triangular lattice structure) is straightforward. A variant of perfectly matched layers (PML) [8] is adopted for simu-

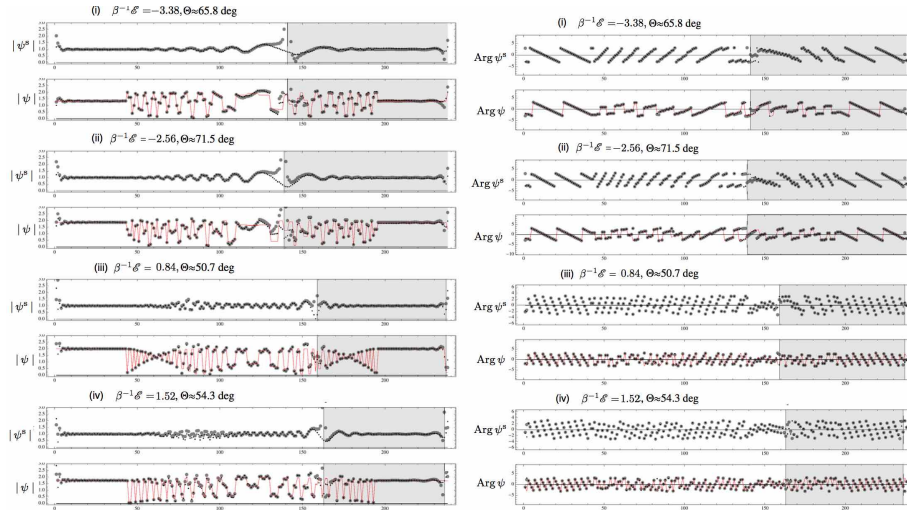


Figure 13: $|\psi^s|$ and $|\psi|$ (left) and $\arg \psi^s$ and $\arg \psi$ (right) on a discrete semi-circular contour as shown in Fig. 12. In all plots, $R_\infty = 40.6$, $N_{\text{grid}} = 71$, $N_{\text{pml}} = 58$ as stated in Fig. 12.

lation of an ‘infinite’ domain (see also [107] and [112]). The probability density $|\psi|^2$ is plotted in Fig. 5 and Fig. 7 for $\mathfrak{S}_{\bullet\bullet}$ and $\mathfrak{T}_{\bullet\bullet}$, respectively. Similar results are also provided in Fig. 12 and Fig. 14 for $\mathfrak{S}_{\bullet\bullet}$ and $\mathfrak{T}_{\bullet\bullet}$, respectively. The numerical solution, displayed in Fig. 12 and Fig. 14, is also compared with the asymptotic approximation (4.2a) of (3.2) for $\mathfrak{S}_{\bullet\bullet}$ and $\mathfrak{T}_{\bullet\bullet}$, respectively. The modulus and argument of wavefunction at every site located on a (fixed) circular contour (as shown in Fig. 12 and Fig. 14) has been calculated (traversed counter-clockwise from (0, 1) labelled 1 and other sites labeled incrementally). These respective results are shown in Fig. 13 and Fig. 15. As expected based on the low energy approximation, since the kernel (1.11b) approaches 1, a ‘flat’ surface (implying only the geometric aspect of specular scattering) behaviour is confirmed by parts (i) of Fig. 13 and Fig. 15 (the slight deviations are attributed to imperfect absorbing boundary on the finite grid).

6 Discussion

In the spirit of earlier works [146, 122, 41, 79, 141, 142, 143, 69, 118, 68] on electron scattering from rough surface in metals, the analysis presented in this paper can be applied in practical situations by taking appropriate convolution using the differential scattering cross section to obtain a general specular parameter. A simple model such as that analyzed in this paper, leads to an exact expression for the dependence of the scattered wavefunction on the incident wavenumber and angle of incidence of the bulk electron. Such analysis is an-

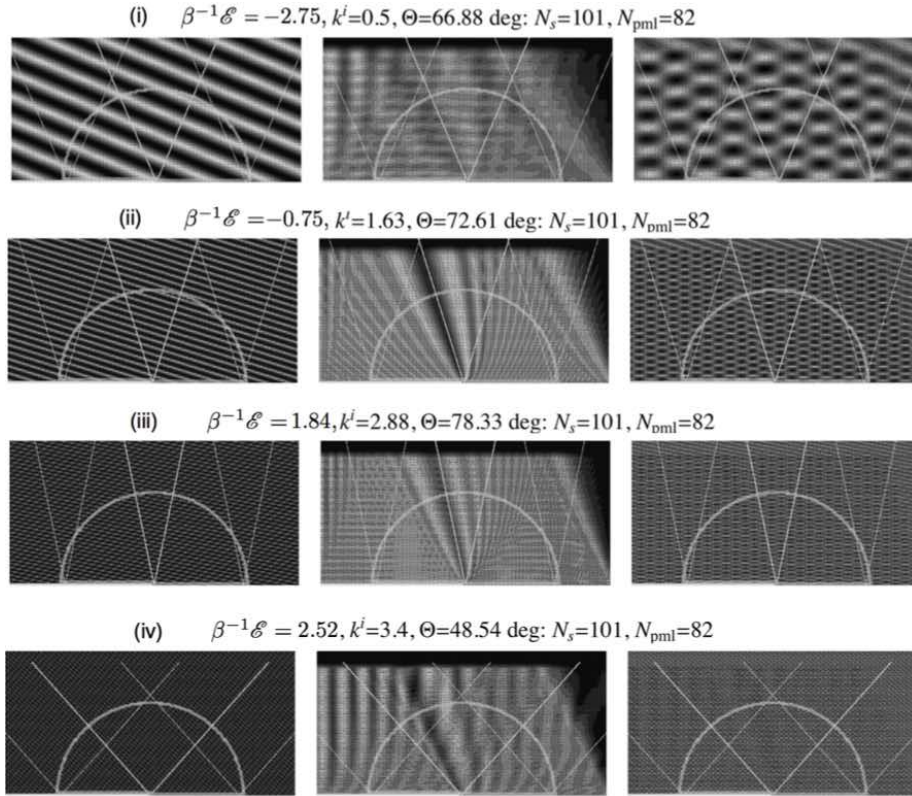


Figure 14: Incident $\text{Re}\psi^{\text{inc}}$ (left), scattered $|\psi^s|$ (center), and $\text{Re}\psi$ (right) wavefunction for the semi-infinite triangular lattice structure with step $\mathfrak{T}_{\bullet\bullet}$.

anticipated to be crucial in a theoretical framework for rough surfaces containing either a random distribution of steps or a specific structure of steps [71]. For instance, the results of this type are hidden behind the extensive analyses based on careful application of statistical/variational methods since several decades for scattering from a statistically rough surface [72, 28, 127, 9, 85] as well as analytical/numerical approximations tackling multiple scattering problems [33, 117, 23]. For a finite number of steps, the geometrical ray approximation of [53, 52, 55, 54] is reckoned highly pertinent.

An essential assumption in the paper is that the electron wavefunction vanishes at the metal boundary [2], which corresponds to the approximation of the surface potential by a rectangular barrier of infinite height. The actual finiteness of the height and region of variation of the surface barrier affects the probability of electron scattering, leading to a smooth decay of the wavefunction within some layer near the surface. To account for the related effects, and to generalize the results of the present paper to more complex types of surface scattering is an open problem at this stage.

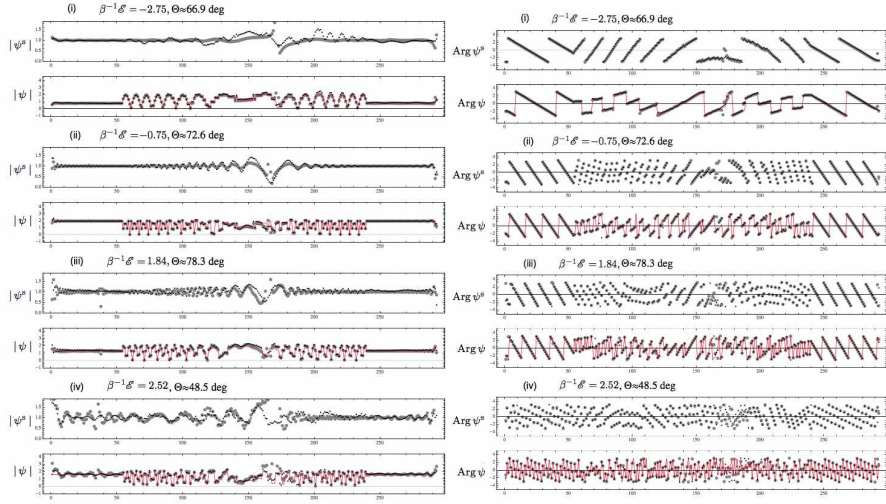


Figure 15: $|\psi^s|$ and $|\psi|$ (left) and $\arg \psi^s$ and $\arg \psi$ (right) on a discrete semi-circular contour as shown in Fig. 14. In all plots, $R_\infty = 53.3$, $N_{\text{grid}} = 101$, $N_{\text{pml}} = 82$ as shown in Fig. 14.

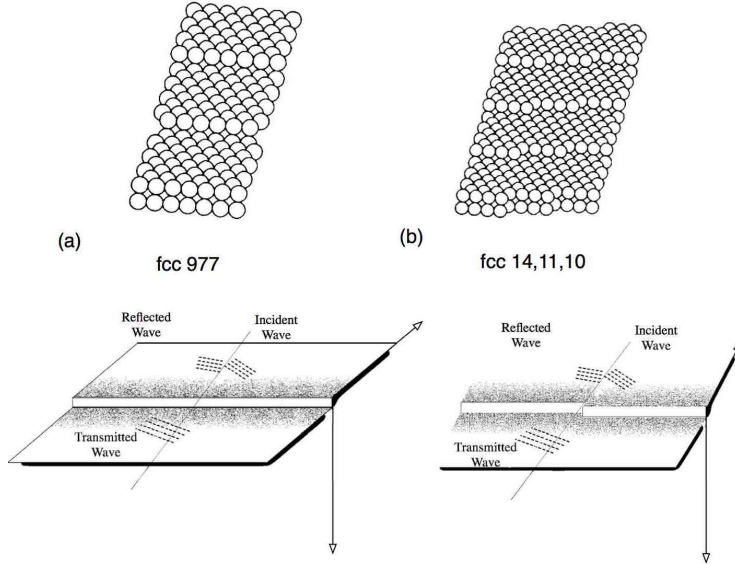


Figure 16: Semi-infinite half space with step [124]. Incident surface state electron schematically shown.

The evolution of wave packets across steps on surfaces also involves inherently several challenges in a more general framework [78, 21]. For surface elec-

tronic states as well, the analysis has an additional relevance based on the occurrence of surface bands, but more realistic model is wanting, hence this is deferred for another study in future. If the crystal surface is misoriented from the low-index plane by a small angle, on the atomic scale, such a surface, called a stepped or vicinal surface, is composed conventionally of terraces separated by steps of monatomic height, which may also have kinks in them (Fig. 16 top and schematic below for a formulation similar to this paper). [102] demonstrated that monoatomic steps on vicinal Cu(111) surfaces act as repulsive barriers for free-electron-like, 2D surface states. The generalization of the results presented in this paper to such situation is an interesting vista that needs to be explored.

Last but not the last the exact solution presented serves some recent interests hinged on the possible analytic solutions for quantum wells using the discrete Schrödinger equation [13], tight-binding models on semi-infinite lattices [133, 119, 145, 134], Bloch wave scattering [80, 147, 83, 140], as well as discrete nature of several interesting wave phenomena at nanoscale [26, 93, 88].

7 Concluding remarks

Surface scattering is conventionally described by the well documented theoretical framework developed by Fuchs [31] and Sondheimer [126], and later modified (for example, [98]) in different contexts to take into account the effects of surface roughness. This paper attempts to understand the same from a simplistic viewpoint, based on a tight-binding approximation, and presents an analysis of electronic wave scattering by an atomic step discontinuity [16] on the boundary of the square lattice half-plane and triangular lattice half-plane. The mathematical problem and technique is similar to that employed by [116] which are presented in the context of physically different problem. The extension to wider steps (multiple atomic layers) brings many more complicated aspects of the mathematical analysis, besides an anticipated reliance on numerics to a much greater extent. In the context of modern technological needs [1], understanding the role of defects in the transport properties of graphene is central to realizing future electronics based on carbon [100] and molecules [132]. Hence, an extension of the analysis presented in this paper to more realistic, and technologically relevant structures in the current scenario, such as honeycomb structure [109, 113], has been planned and shall be presented elsewhere. The same statement holds for the analysis of corresponding two dimensional lattice waveguides [81] with a step discontinuity on one or both boundary following [114]. Such detailed analysis of the size effect on (ballistic) electric conductivity (or resistance) based on surface (boundary) scattering for thin ‘ribbons’ is currently under investigation and shall be presented in future elsewhere.

References

- [1] D. M. Adams et al. “Charge transfer on the nanoscale: current status”. In: *The Journal of Physical Chemistry B* 107.28 (2003), pp. 6668–6697.
- [2] A. F. Andreev. “Interaction of conduction electrons with a metal surface”. In: *Soviet Physics Uspekhi* 14.5 (1972), p. 609. URL: <http://stacks.iop.org/0038-5670/14/i=5/a=R04>.
- [3] E. R. Andrew. “The Size-Variation of Resistivity for Mercury and Tin”. In: *Proceedings of the Physical Society. Section A* 62.2 (1949), p. 77. URL: <http://stacks.iop.org/0370-1298/62/i=2/a=301>.
- [4] G. R. Baldock. “Electronic bound states at the surface of a metal”. In: *Mathematical Proceedings of the Cambridge Philosophical Society* 48.3 (1952), 457?469. DOI: [10.1017/S0305004100027870](https://doi.org/10.1017/S0305004100027870).
- [5] E. Baskin and M. Entin. “Electron Scattering and the Conductivity of a Film with Surface Defects”. In: *Soviet Physics JETP* 30.2 (1970), p. 252.
- [6] S. Bauer and C. A. Bobisch. “Nanoscale electron transport at the surface of a topological insulator”. In: *Nature communications* 7 (2016).
- [7] C. Beenakker and H. van Houten. “Quantum transport in semiconductor nanostructures”. In: *Solid state physics* 44 (1991), pp. 1–228.
- [8] J.-P. Berenger. “A perfectly matched layer for the absorption of electromagnetic waves”. In: *J. Comp. Phys.* 114 (1994), pp. 185–200.
- [9] J. F. Bird. “Analysis of all-frequency variational behavior of the Kirchhoff approximation for a classic surface-scattering model”. In: *J. Opt. Soc. Am. A* 2.6 (June 1985), pp. 945–953. DOI: [10.1364/JOSAA.2.000945](https://doi.org/10.1364/JOSAA.2.000945). URL: <http://josaa.osa.org/abstract.cfm?URI=josaa-2-6-945>.
- [10] R. R. Biswas and A. V. Balatsky. “Scattering from surface step edges in strong topological insulators”. In: *Physical Review B* 83.7 (2011), p. 075439.
- [11] F. Bloch. “Über die quantenmechanik der elektronen in kristallgittern”. In: *Zeitschrift für Physik A Hadrons and Nuclei* 52.7 (1929), pp. 555–600.
- [12] M. Born and E. Wolf. *Principles of Optics*. Cambridge, U.K.: Cambridge University Press, 1999.
- [13] T. B. Boykin and G. Klimeck. “The discretized Schrödinger equation and simple models for semiconductor quantum wells”. In: *European Journal of Physics* 25.4 (2004), p. 503. URL: <http://stacks.iop.org/0143-0807/25/i=4/a=006>.
- [14] L. Brillouin. *Wave propagation in periodic structures; electric filters and crystal lattices*. New York: Dover Publications, 1953.

- [15] L. Bürgi et al. “Confinement of Surface State Electrons in Fabry-Pérot Resonators”. In: *Phys. Rev. Lett.* 81 (24 Dec. 1998), pp. 5370–5373. DOI: [10.1103/PhysRevLett.81.5370](https://doi.org/10.1103/PhysRevLett.81.5370). URL: <http://link.aps.org/doi/10.1103/PhysRevLett.81.5370>.
- [16] C. Busse et al. “Atomic Layer Growth on Al(111) by Ion Bombardment”. In: *Phys. Rev. Lett.* 85 (2 July 2000), pp. 326–329. DOI: [10.1103/PhysRevLett.85.326](https://doi.org/10.1103/PhysRevLett.85.326). URL: <http://link.aps.org/doi/10.1103/PhysRevLett.85.326>.
- [17] J. Callaway. *Energy band theory*. Pure and applied physics. New York: Academic Press, 1964.
- [18] R. G. Chambers. “The Conductivity of Thin Wires in a Magnetic Field”. In: *Proceedings of the Royal Society of London A: Mathematical, Physical and Engineering Sciences* 202.1070 (1950), pp. 378–394. DOI: [10.1098/rspa.1950.0107](https://doi.org/10.1098/rspa.1950.0107). URL: <http://rspa.royalsocietypublishing.org/content/202/1070/378>.
- [19] B. R. Cooper and A. J. Bennett. “Theory of Electronic Properties of Thin Films of *d*-Band Metals”. In: *Phys. Rev. B* 1 (12 June 1970), pp. 4654–4667. DOI: [10.1103/PhysRevB.1.4654](https://doi.org/10.1103/PhysRevB.1.4654). URL: <https://link.aps.org/doi/10.1103/PhysRevB.1.4654>.
- [20] M. Crommie, C. Lutz, and D. Eigler. “Imaging standing waves in a two-dimensional electron gas”. In: *Nature* 363.6429 (1993), pp. 524–527.
- [21] F. Cuevas, S. Curilef, and A. Plastino. “Spread of highly localized wavepacket in the tight-binding lattice: Entropic and information-theoretical characterization”. In: *Annals of Physics* 326.10 (2011), pp. 2834–2844.
- [22] S. Davison and J. Levine. “Surface States”. In: *Solid State Physics* 25 (1970), pp. 1–149. DOI: [http://dx.doi.org/10.1016/S0081-1947\(08\)60008-9](http://dx.doi.org/10.1016/S0081-1947(08)60008-9). URL: <http://www.sciencedirect.com/science/article/pii/S0081194708600089>.
- [23] J. A. Desanto and G. S. Brown. “Analytical Techniques for Multiple Scattering from Rough Surfaces”. In: *Progress in Optics* 23 (1986), pp. 1–62.
- [24] V. K. Dugaev and M. I. Katsnelson. “Edge scattering of electrons in graphene: Boltzmann equation approach to the transport in graphene nanoribbons and nanodisks”. In: *Phys. Rev. B* 88 (23 Dec. 2013), p. 235432. DOI: [10.1103/PhysRevB.88.235432](https://doi.org/10.1103/PhysRevB.88.235432). URL: <http://link.aps.org/doi/10.1103/PhysRevB.88.235432>.
- [25] E. N. Economou. *Green’s functions in quantum physics*. second. Berlin: Springer, 1983.
- [26] H. Eisenberg et al. “Discrete spatial optical solitons in waveguide arrays”. In: *Physical Review Letters* 81.16 (1998), p. 3383.
- [27] A. Erdélyi. “Asymptotic representations of Fourier integrals and the method of stationary phase”. In: *Journal of the Society for Industrial and Applied Mathematics* 3.1 (1955), pp. 17–27.

- [28] I. M. F. F. G. Bass and D. ter Haar (Auth.) *Wave Scattering from Statistically Rough Surfaces*. 0th ed. Pergamon Press, 1979.
- [29] L. B. Felsen and N. Marcuvitz. *Radiation and Scattering of Waves*. Englewood Cliffs NJ: Prentice-Halls, 1973.
- [30] G. Fishman and D. Calecki. “Influence of surface roughness on the conductivity of metallic and semiconducting quasi-two-dimensional structures”. In: *Phys. Rev. B* 43 (14 May 1991), pp. 11581–11585. DOI: [10.1103/PhysRevB.43.11581](https://doi.org/10.1103/PhysRevB.43.11581). URL: <http://link.aps.org/doi/10.1103/PhysRevB.43.11581>.
- [31] K. Fuchs. “The conductivity of thin metallic films according to the electron theory of metals”. In: *Mathematical Proceedings of the Cambridge Philosophical Society* 34.1 (Jan. 1938), pp. 100–108. DOI: [10.1017/S0305004100019952](https://doi.org/10.1017/S0305004100019952). URL: <https://www.cambridge.org/core/article/div-class-title-conductivity-of-thin-metallic-films-according-to-the-electron-theory-of-metals-div/B67FD21662E4DC38745343C4CF8455FD>.
- [32] Y. Q. Gao and R. Marcus. “Application of the z-transform to composite materials”. In: *The Journal of Chemical Physics* 115.21 (2001), pp. 9929–9934.
- [33] N. Garcia, V. Celli, and M. Nieto-Vesperinas. “Exact multiple scattering of waves from random rough surfaces”. In: *Optics Communications* 30.3 (1979), pp. 279–281.
- [34] E. T. Goodwin. “Electronic states at the surfaces of crystals. I. The approximation of nearly free electrons”. In: *Mathematical Proceedings of the Cambridge Philosophical Society* 35.02 (1939), pp. 205–220.
- [35] E. T. Goodwin. “Electronic states at the surfaces of crystals. II. The approximation of tight binding: finite linear chain of atoms”. In: *Mathematical Proceedings of the Cambridge Philosophical Society* 35.2 (1939), pp. 221–231.
- [36] E. T. Goodwin. “Electronic states at the surfaces of crystals: III. The approximation of tight binding: further extensions”. In: *Mathematical Proceedings of the Cambridge Philosophical Society* 35.2 (1939), pp. 232–241.
- [37] E. T. Goodwin. “Electronic states at the surfaces of crystals: IV. The activation of adsorbed atoms by surface electrons”. In: *Mathematical Proceedings of the Cambridge Philosophical Society* 35.3 (1939), pp. 474–484.
- [38] R. L. Graham et al. “Resistivity dominated by surface scattering in sub-50 nm Cu wires”. In: *Applied Physics Letters* 96.4 (2010), p. 042116. DOI: [10.1063/1.3292022](https://doi.org/10.1063/1.3292022). URL: <http://dx.doi.org/10.1063/1.3292022>.
- [39] R. F. Greene. “Angular Dependence of Surface Scattering and Surface Mobility Cusp”. In: *Phys. Rev.* 141 (2 Jan. 1966), pp. 690–692. DOI: [10.1103/PhysRev.141.690](https://doi.org/10.1103/PhysRev.141.690). URL: <http://link.aps.org/doi/10.1103/PhysRev.141.690>.

- [40] R. F. Greene. “Boundary Conditions for Electron Distributions at Crystal Surfaces”. In: *Phys. Rev.* 141 (2 Jan. 1966), pp. 687–689. DOI: [10.1103/PhysRev.141.687](https://doi.org/10.1103/PhysRev.141.687). URL: <http://link.aps.org/doi/10.1103/PhysRev.141.687>.
- [41] R. F. Greene and R. W. O’Donnell. “Scattering of Conduction Electrons by Localized Surface Charges”. In: *Phys. Rev.* 147 (2 July 1966), pp. 599–602. DOI: [10.1103/PhysRev.147.599](https://doi.org/10.1103/PhysRev.147.599). URL: <http://link.aps.org/doi/10.1103/PhysRev.147.599>.
- [42] R. Greene. “Surface transport”. In: *Surface Science* 2 (1964), pp. 101–113. DOI: [http://dx.doi.org/10.1016/0039-6028\(64\)90048-2](https://doi.org/10.1016/0039-6028(64)90048-2). URL: <http://www.sciencedirect.com/science/article/pii/S0039602864900482>.
- [43] Y. Hasegawa and P. Avouris. “Direct observation of standing wave formation at surface steps using scanning tunneling spectroscopy”. In: *Phys. Rev. Lett.* 71 (7 Aug. 1993), pp. 1071–1074. DOI: [10.1103/PhysRevLett.71.1071](https://doi.org/10.1103/PhysRevLett.71.1071). URL: <http://link.aps.org/doi/10.1103/PhysRevLett.71.1071>.
- [44] R. Henriquez et al. “Electron scattering at surfaces and grain boundaries in thin Au films”. In: *Applied Surface Science* 273 (2013), pp. 315–323. DOI: [http://dx.doi.org/10.1016/j.apsusc.2013.02.037](https://doi.org/10.1016/j.apsusc.2013.02.037). URL: <http://www.sciencedirect.com/science/article/pii/S0169433213003450>.
- [45] J. C. Hensel et al. “Specular Boundary Scattering and Electrical Transport in Single-Crystal Thin Films of CoSi₂”. In: *Phys. Rev. Lett.* 54 (16 Apr. 1985), pp. 1840–1843. DOI: [10.1103/PhysRevLett.54.1840](https://doi.org/10.1103/PhysRevLett.54.1840). URL: <https://link.aps.org/doi/10.1103/PhysRevLett.54.1840>.
- [46] H. Hoffmann, J. Vancea, and U. Jacob. “Surface scattering of electrons in metals”. In: *Thin Solid Films* 129.3 4 (1985), pp. 181–193. DOI: [http://dx.doi.org/10.1016/0040-6090\(85\)90045-8](https://doi.org/10.1016/0040-6090(85)90045-8). URL: <http://www.sciencedirect.com/science/article/pii/0040609085900458>.
- [47] T. Horiguchi. “Lattice Green’s functions for the triangular and honeycomb lattices”. In: *J. Math. Phys.* 13 (1972), pp. 1411–1419.
- [48] E. Hückel. “Zur Quantentheorie der Doppelbindung”. In: *Zeitschrift für Physik* 60.7 (1930). On the quantum theory of double bonding, pp. 423–456. DOI: [10.1007/BF01341254](https://doi.org/10.1007/BF01341254). URL: <http://dx.doi.org/10.1007/BF01341254>.
- [49] E. I. Jury. *Theory and application of the z-transform method*. New York: John Wiley, 1964.
- [50] E. Kaxiras. *Atomic and Electronic Structure of Solids*. Cambridge University Press, 2003.

- [51] Y. Ke et al. “Resistivity of thin Cu films with surface roughness”. In: *Phys. Rev. B* 79 (15 Apr. 2009), p. 155406. DOI: [10.1103/PhysRevB.79.155406](https://doi.org/10.1103/PhysRevB.79.155406). URL: <http://link.aps.org/doi/10.1103/PhysRevB.79.155406>.
- [52] J. B. Keller. “Diffraction by an Aperture”. In: *Journal of Applied Physics* 28.4 (1957), pp. 426–444. DOI: [10.1063/1.1722767](https://doi.org/10.1063/1.1722767). URL: <http://dx.doi.org/10.1063/1.1722767>.
- [53] J. B. Keller. “Geometrical Theory of Diffraction”. In: *J. Opt. Soc. Am.* 52.2 (Feb. 1962), pp. 116–130. DOI: [10.1364/JOSA.52.000116](https://doi.org/10.1364/JOSA.52.000116). URL: <http://www.osapublishing.org/abstract.cfm?URI=josa-52-2-116>.
- [54] J. B. Keller. “Rays, Waves and Asymptotics”. In: *Classical and Modern Diffraction Theory* (2016), p. 67.
- [55] J. B. Keller, R. M. Lewis, and B. D. Seckler. “Diffraction by an Aperture. II”. In: *Journal of Applied Physics* 28.5 (1957), pp. 570–579. DOI: [10.1063/1.1722805](https://doi.org/10.1063/1.1722805). URL: <http://dx.doi.org/10.1063/1.1722805>.
- [56] S. Kim et al. “Surface Scattering via Bulk Continuum States in the 3D Topological Insulator Bi_2Se_3 ”. In: *Phys. Rev. Lett.* 107 (5 July 2011), p. 056803. DOI: [10.1103/PhysRevLett.107.056803](https://doi.org/10.1103/PhysRevLett.107.056803). URL: <http://link.aps.org/doi/10.1103/PhysRevLett.107.056803>.
- [57] C. Kittel. *Introduction to solid state physics*. Wiley, 1971. URL: <https://books.google.co.in/books?id=-wBRAAAAMAAJ>.
- [58] N. Knorr et al. “Kondo Effect of Single Co Adatoms on Cu Surfaces”. In: *Phys. Rev. Lett.* 88 (9 Feb. 2002), p. 096804. DOI: [10.1103/PhysRevLett.88.096804](https://doi.org/10.1103/PhysRevLett.88.096804). URL: <http://link.aps.org/doi/10.1103/PhysRevLett.88.096804>.
- [59] J. F. Koch and T. E. Murray. “Electron Scattering at a Rough Surface”. In: *Phys. Rev.* 186 (3 Oct. 1969), pp. 722–727. DOI: [10.1103/PhysRev.186.722](https://doi.org/10.1103/PhysRev.186.722). URL: <http://link.aps.org/doi/10.1103/PhysRev.186.722>.
- [60] J. Koringa. “On the calculation of the energy of a Bloch wave in a metal”. In: *Physica* 13.6-7 (1947), pp. 392–400. DOI: [10.1016/0031-8914\(47\)90013-X](https://doi.org/10.1016/0031-8914(47)90013-X). URL: <http://www.sciencedirect.com/science/article/pii/003189144790013X>.
- [61] G. F. Koster and J. Slater. “Wave functions for impurity levels”. In: *Physical Review* 95.5 (1954), p. 1167.
- [62] J. Koutecký. “Quantum Chemistry of Crystal Surfaces”. In: *Advances in Chemical Physics*. John Wiley & Sons, Inc., 2007, pp. 85–168. DOI: [10.1002/9780470143551.ch2](https://doi.org/10.1002/9780470143551.ch2). URL: <http://dx.doi.org/10.1002/9780470143551.ch2>.
- [63] J. Koutecký. “Contribution to the Theory of the Surface Electronic States in the One-Electron Approximation”. In: *Phys. Rev.* 108 (1 Oct. 1957), pp. 13–18. DOI: [10.1103/PhysRev.108.13](https://doi.org/10.1103/PhysRev.108.13). URL: <https://link.aps.org/doi/10.1103/PhysRev.108.13>.

- [64] R. d. L. Kronig and W. Penney. “Quantum mechanics of electrons in crystal lattices”. In: *Proceedings of the Royal Society of London A: Mathematical, Physical and Engineering Sciences* 130.814 (1931), pp. 499–513.
- [65] L. Künne. “Berechnung von oberflächenzuständen für einige kristalltypen nach der tight binding methode”. In: *Czechoslovak Journal of Physics B* 17.10 (Oct. 1967), pp. 894–905. DOI: [10.1007/BF01691641](https://doi.org/10.1007/BF01691641). URL: <https://doi.org/10.1007/BF01691641>.
- [66] O. Kurnosikov et al. “Long-Range Electron Interferences at a Metal Surface Induced by Buried Nanocavities”. In: *Phys. Rev. Lett.* 102 (6 Feb. 2009), p. 066101. DOI: [10.1103/PhysRevLett.102.066101](https://doi.org/10.1103/PhysRevLett.102.066101). URL: <http://link.aps.org/doi/10.1103/PhysRevLett.102.066101>.
- [67] D. C. Larson. “Size dependent electrical conduction in thin metal films and wires”. In: *Physics of Thin Films: Advances in Research and Development*. Ed. by M. H. Francombe and R. W. Hoffman. Physics of Thin Films 6. Academic Press, 1971, pp. -.
- [68] R. Lenk and A. Knabchen. “The roughness-induced classical size effect in thin films”. In: *Journal of Physics: Condensed Matter* 5.36 (1993), p. 6563. URL: <http://stacks.iop.org/0953-8984/5/i=36/a=011>.
- [69] D. Lessie. “Multiple scattering of conduction electrons at disordered metal surfaces”. In: *Phys. Rev. B* 20 (6 Sept. 1979), pp. 2491–2505. DOI: [10.1103/PhysRevB.20.2491](https://doi.org/10.1103/PhysRevB.20.2491). URL: <http://link.aps.org/doi/10.1103/PhysRevB.20.2491>.
- [70] J. D. Louck. “Exact Normal Modes of Oscillation of a Linear Chain of Identical Particles”. In: *American Journal of Physics* 30.8 (1962), pp. 585–590. DOI: [http://dx.doi.org/10.1119/1.1942116](https://doi.org/10.1119/1.1942116). URL: <http://scitation.aip.org/content/aapt/journal/ajp/30/8/10.1119/1.1942116>.
- [71] T.-M. Lu and M. Lagally. “Diffraction from surfaces with randomly distributed steps”. In: *Surface Science* 120.1 (1982), pp. 47–66. DOI: [http://dx.doi.org/10.1016/0039-6028\(82\)90274-6](https://doi.org/10.1016/0039-6028(82)90274-6). URL: <http://www.sciencedirect.com/science/article/pii/0039602882902746>.
- [72] A. A. Maradudin and D. L. Mills. “Scattering and absorption of electromagnetic radiation by a semi-infinite medium in the presence of surface roughness”. In: *Phys. Rev. B* 11 (4 Feb. 1975), pp. 1392–1415. DOI: [10.1103/PhysRevB.11.1392](https://doi.org/10.1103/PhysRevB.11.1392). URL: <http://link.aps.org/doi/10.1103/PhysRevB.11.1392>.
- [73] R. Marcus. “Tight-binding approximation for semi-infinite solids. Application of a transform method and of delta function normalization”. In: *The Journal of chemical physics* 98.7 (1993), pp. 5604–5611.
- [74] H. Marom and M. Eizenberg. “The effect of surface roughness on the resistivity increase in nanometric dimensions”. In: *Journal of Applied Physics* 99.12 (2006), p. 123705. DOI: [10.1063/1.2204349](https://doi.org/10.1063/1.2204349). URL: <http://dx.doi.org/10.1063/1.2204349>.

- [75] I. Matsuda et al. “Electrical resistance of a monatomic step on a crystal surface”. In: *Physical review letters* 93.23 (2004), p. 236801.
- [76] A. F. Mayadas and M. Shatzkes. “Electrical-Resistivity Model for Polycrystalline Films: the Case of Arbitrary Reflection at External Surfaces”. In: *Phys. Rev. B* 1 (4 Feb. 1970), pp. 1382–1389. DOI: [10.1103/PhysRevB.1.1382](https://doi.org/10.1103/PhysRevB.1.1382). URL: <https://link.aps.org/doi/10.1103/PhysRevB.1.1382>.
- [77] A. E. Meyerovich and I. V. Ponomarev. “Surface roughness and size effects in quantized films”. In: *Phys. Rev. B* 65 (15 Mar. 2002), p. 155413. DOI: [10.1103/PhysRevB.65.155413](https://doi.org/10.1103/PhysRevB.65.155413). URL: <http://link.aps.org/doi/10.1103/PhysRevB.65.155413>.
- [78] A. E. Miroschnichenko, S. Flach, and Y. S. Kivshar. “Fano resonances in nanoscale structures”. In: *Rev. Mod. Phys.* 82 (3 Aug. 2010), pp. 2257–2298. DOI: [10.1103/RevModPhys.82.2257](https://doi.org/10.1103/RevModPhys.82.2257). URL: <https://link.aps.org/doi/10.1103/RevModPhys.82.2257>.
- [79] R. M. More and D. Lessie. “Specular Reflection of Conduction Electrons at a Metal Surface”. In: *Phys. Rev. B* 8 (6 Sept. 1973), pp. 2527–2535. DOI: [10.1103/PhysRevB.8.2527](https://doi.org/10.1103/PhysRevB.8.2527). URL: <http://link.aps.org/doi/10.1103/PhysRevB.8.2527>.
- [80] G. J. Morgan. “Bloch waves and scattering by impurities”. In: *Proceedings of the Physical Society* 89.2 (1966), p. 365. URL: <http://stacks.iop.org/0370-1328/89/i=2/a=316>.
- [81] K. Na and L. E. Reichl. “Electron Conductance and Lifetimes in a Ballistic Electron Waveguide”. In: *Journal of Statistical Physics* 92.3 (Aug. 1998), pp. 519–542. DOI: [10.1023/A:1023032420009](https://doi.org/10.1023/A:1023032420009). URL: <https://doi.org/10.1023/A:1023032420009>.
- [82] Y. Namba. “Resistivity and Temperature Coefficient of Thin Metal Films with Rough Surface”. In: *Japanese Journal of Applied Physics* 9.11 (1970), p. 1326. URL: <http://stacks.iop.org/1347-4065/9/i=11/a=1326>.
- [83] R. G. Newton. “Bloch-wave scattering by crystal defects”. In: *Journal of Mathematical Physics* 32.2 (1991), pp. 551–560. DOI: [10.1063/1.529392](https://doi.org/10.1063/1.529392). URL: <http://dx.doi.org/10.1063/1.529392>.
- [84] B. Noble. *Methods based on the Wiener–Hopf technique*. London: Pergamon Press, 1958.
- [85] J. A. Ogilvy and H. M. Merklinger. “Theory of wave scattering from random rough surfaces”. In: *The Journal of the Acoustical Society of America* 90.6 (1991), pp. 3382–3382.
- [86] R. Ohmann et al. “Quantum coherence of bulk electrons on metals revealed by scanning tunneling spectroscopy”. In: *Phys. Rev. B* 89 (20 May 2014), p. 205433. DOI: [10.1103/PhysRevB.89.205433](https://doi.org/10.1103/PhysRevB.89.205433). URL: <http://link.aps.org/doi/10.1103/PhysRevB.89.205433>.
- [87] K. Oura et al. *Surface Science: An Introduction*. 1st ed. Advanced Texts in Physics. Springer-Verlag Berlin Heidelberg, 2003.

- [88] E. Ozbay. “Plasmonics: merging photonics and electronics at nanoscale dimensions”. In: *science* 311.5758 (2006), pp. 189–193.
- [89] G. Palasantzas and J. Barnas. “Surface-roughness fractality effects in electrical conductivity of single metallic and semiconducting films”. In: *Phys. Rev. B* 56 (12 Sept. 1997), pp. 7726–7731. DOI: [10.1103/PhysRevB.56.7726](https://doi.org/10.1103/PhysRevB.56.7726). URL: <http://link.aps.org/doi/10.1103/PhysRevB.56.7726>.
- [90] A. V. de Parga et al. “Quantum oscillations in surface properties”. In: *Surface Science* 603.10 12 (2009). Special Issue of Surface Science dedicated to Prof. Dr. Dr. h.c. mult. Gerhard Ertl, Nobel-Laureate in Chemistry 2007, pp. 1389–1396. DOI: <http://dx.doi.org/10.1016/j.susc.2008.08.039>. URL: <http://www.sciencedirect.com/science/article/pii/S0039602809000739>.
- [91] J. E. Parrott. “A new theory of the size effect in electrical conduction”. In: *Proceedings of the Physical Society* 85.6 (1965), p. 1143. URL: <http://stacks.iop.org/0370-1328/85/i=6/a=312>.
- [92] J. I. Pascual et al. “Bulk Electronic Structure of Metals Resolved with Scanning Tunneling Microscopy”. In: *Phys. Rev. Lett.* 96 (4 Feb. 2006), p. 046801. DOI: [10.1103/PhysRevLett.96.046801](https://doi.org/10.1103/PhysRevLett.96.046801). URL: <http://link.aps.org/doi/10.1103/PhysRevLett.96.046801>.
- [93] T. Pertsch et al. “Anomalous refraction and diffraction in discrete optical systems”. In: *Physical review letters* 88.9 (2002), p. 093901.
- [94] L. Petersen et al. “Screening waves from steps and defects on Cu(111) and Au(111) imaged with STM: Contribution from bulk electrons”. In: *Phys. Rev. B* 58 (11 Sept. 1998), pp. 7361–7366. DOI: [10.1103/PhysRevB.58.7361](https://doi.org/10.1103/PhysRevB.58.7361). URL: <http://link.aps.org/doi/10.1103/PhysRevB.58.7361>.
- [95] D. G. Pettifor. *Bonding and Structure of Molecules and Solids*. Oxford University Press, USA, 1995.
- [96] J. Pollmann. “Defects at surfaces and interfaces: A scattering theoretical approach”. In: *Solid State Communications* 34.7 (1980), pp. 587–590.
- [97] J. Pollmann. “On the electronic structure of semiconductor surfaces, interfaces and defects at surfaces or interfaces”. In: *Festkörperprobleme 20*. Springer, 1979, pp. 117–175.
- [98] S. M. Rossnagel and T. S. Kuan. “Alteration of Cu conductivity in the size effect regime”. In: *Journal of Vacuum Science & Technology B: Microelectronics and Nanometer Structures Processing, Measurement, and Phenomena* 22.1 (2004), pp. 240–247. DOI: [10.1116/1.1642639](https://doi.org/10.1116/1.1642639). URL: <http://avs.scitation.org/doi/abs/10.1116/1.1642639>.
- [99] R. Rurali. “Colloquium: Structural, electronic, and transport properties of silicon nanowires”. In: *Reviews of Modern Physics* 82.1 (2010), p. 427.

- [100] G. M. Rutter et al. “Scattering and Interference in Epitaxial Graphene”. In: *Science* 317.5835 (2007), pp. 219–222. DOI: [10.1126/science.1142882](https://doi.org/10.1126/science.1142882). URL: <http://science.sciencemag.org/content/317/5835/219>.
- [101] J. Sambles. “The resistivity of thin metal films — Some critical remarks”. In: *Thin Solid Films* 106.4 (1983), pp. 321–331. DOI: [http://dx.doi.org/10.1016/0040-6090\(83\)90344-9](http://dx.doi.org/10.1016/0040-6090(83)90344-9). URL: <http://www.sciencedirect.com/science/article/pii/0040609083903449>.
- [102] O. Sánchez et al. “Lateral confinement of surface states on stepped Cu(111)”. In: *Phys. Rev. B* 52 (11 Sept. 1995), pp. 7894–7897. DOI: [10.1103/PhysRevB.52.7894](https://doi.org/10.1103/PhysRevB.52.7894). URL: <http://link.aps.org/doi/10.1103/PhysRevB.52.7894>.
- [103] M. Schmeits, A. Mazur, and J. Pollmann. “Scattering-theoretical method for relaxed and reconstructed surfaces with applications to GaAs(110) and Si(100)-(2×1)”. In: *Phys. Rev. B* 27 (8 Apr. 1983), pp. 5012–5031. DOI: [10.1103/PhysRevB.27.5012](https://doi.org/10.1103/PhysRevB.27.5012). URL: <https://link.aps.org/doi/10.1103/PhysRevB.27.5012>.
- [104] M. Schmid, S. Crampin, and P. Varga. “{STM} and {STS} of bulk electron scattering by subsurface objects”. In: *Journal of Electron Spectroscopy and Related Phenomena* 109.1 2 (2000), pp. 71–84. DOI: [http://dx.doi.org/10.1016/S0368-2048\(00\)00108-0](http://dx.doi.org/10.1016/S0368-2048(00)00108-0). URL: <http://www.sciencedirect.com/science/article/pii/S0368204800001080>.
- [105] K. Schouteden, P. Lievens, and C. Van Haesendonck. “Fourier-transform scanning tunneling microscopy investigation of the energy versus wave vector dispersion of electrons at the Au(111) surface”. In: *Phys. Rev. B* 79 (19 May 2009), p. 195409. DOI: [10.1103/PhysRevB.79.195409](https://doi.org/10.1103/PhysRevB.79.195409). URL: <http://link.aps.org/doi/10.1103/PhysRevB.79.195409>.
- [106] W. Shaban and B. Vainberg. “Radiation conditions for the difference Schrödinger operators”. In: *Applicable Analysis* 80 (2001), pp. 525–556.
- [107] B. L. Sharma. “Diffraction of waves on square lattice by semi-infinite crack”. In: *SIAM Journal on Applied Mathematics* 75.3 (2015), pp. 1171–1192. DOI: [10.1137/140985093](https://doi.org/10.1137/140985093). URL: <http://dx.doi.org/10.1137/140985093>.
- [108] B. L. Sharma. “Diffraction of waves on square lattice by semi-infinite rigid constraint”. In: *Wave Motion* 59 (2015), pp. 52–68. DOI: <http://dx.doi.org/10.1016/j.wavemoti.2015.07.008>. URL: <http://www.sciencedirect.com/science/article/pii/S0165212515001146>.
- [109] B. L. Sharma. “Discrete Sommerfeld diffraction problems on hexagonal lattice with a zigzag semi-infinite crack and rigid constraint”. In: *Zeitschrift für Angewandte Mathematik und Physik* 66.6 (2015), pp. 3591–3625. DOI: [10.1007/s00033-015-0574-2](https://doi.org/10.1007/s00033-015-0574-2). URL: <http://dx.doi.org/10.1007/s00033-015-0574-2>.

- [110] B. L. Sharma. “Near-tip field for diffraction on square lattice by crack”. In: *SIAM Journal on Applied Mathematics* 75.4 (2015), pp. 1915–1940. DOI: [10.1137/15M1010646](https://doi.org/10.1137/15M1010646). URL: <http://dx.doi.org/10.1137/15M1010646>.
- [111] B. L. Sharma. “Near-tip field for diffraction on square lattice by rigid constraint”. In: *Zeitschrift für Angewandte Mathematik und Physik* 66.5 (2015), pp. 2719–2740. DOI: [10.1007/s00033-015-0508-z](https://doi.org/10.1007/s00033-015-0508-z). URL: <http://dx.doi.org/10.1007/s00033-015-0508-z>.
- [112] B. L. Sharma. “Diffraction of waves on triangular lattice by a semi-infinite rigid constraint and crack”. In: *International Journal of Solids and Structures* 80 (2016), pp. 465–485. DOI: [http://dx.doi.org/10.1016/j.ijsolstr.2015.10.008](https://doi.org/10.1016/j.ijsolstr.2015.10.008). URL: <http://www.sciencedirect.com/science/article/pii/S0020768315004242>.
- [113] B. L. Sharma. “Edge diffraction on triangular and hexagonal lattices: Existence, uniqueness, and finite section”. In: *Wave Motion* 65 (2016), pp. 55–78. DOI: [http://dx.doi.org/10.1016/j.wavemoti.2016.04.005](https://doi.org/10.1016/j.wavemoti.2016.04.005). URL: <http://www.sciencedirect.com/science/article/pii/S0165212516300105>.
- [114] B. L. Sharma. “Wave Propagation in Bifurcated Waveguides of Square Lattice Strips”. In: *SIAM Journal on Applied Mathematics* 76.4 (2016), pp. 1355–1381. DOI: [10.1137/15M1051464](https://doi.org/10.1137/15M1051464). URL: <http://dx.doi.org/10.1137/15M1051464>.
- [115] B. L. Sharma. “On linear waveguides of square and triangular lattice strips: an application of Chebyshev polynomials”. In: *Sādhanā* 42.6 (June 2017), pp. 901–927. DOI: [10.1007/s12046-017-0646-4](https://doi.org/10.1007/s12046-017-0646-4). URL: <http://dx.doi.org/10.1007/s12046-017-0646-4>.
- [116] B. L. Sharma. “On scattering of waves on square lattice half-plane with mixed boundary condition”. In: *Zeitschrift für angewandte Mathematik und Physik* 68.5 (Oct. 2017), p. 120. DOI: [10.1007/s00033-017-0854-0](https://doi.org/10.1007/s00033-017-0854-0). URL: <https://doi.org/10.1007/s00033-017-0854-0>.
- [117] J. Shen and A. A. Maradudin. “Multiple scattering of waves from random rough surfaces”. In: *Phys. Rev. B* 22 (9 Nov. 1980), pp. 4234–4240. DOI: [10.1103/PhysRevB.22.4234](https://link.aps.org/doi/10.1103/PhysRevB.22.4234). URL: <https://link.aps.org/doi/10.1103/PhysRevB.22.4234>.
- [118] S. K. Sinha et al. “X-ray and neutron scattering from rough surfaces”. In: *Phys. Rev. B* 38 (4 Aug. 1988), pp. 2297–2311. DOI: [10.1103/PhysRevB.38.2297](https://link.aps.org/doi/10.1103/PhysRevB.38.2297). URL: <https://link.aps.org/doi/10.1103/PhysRevB.38.2297>.
- [119] H. L. Skriver and N. M. Rosengaard. “Self-consistent Green’s-function technique for surfaces and interfaces”. In: *Phys. Rev. B* 43 (12 Apr. 1991), pp. 9538–9549. DOI: [10.1103/PhysRevB.43.9538](https://link.aps.org/doi/10.1103/PhysRevB.43.9538). URL: <https://link.aps.org/doi/10.1103/PhysRevB.43.9538>.

- [120] J. C. Slater and G. F. Koster. “Simplified LCAO Method for the Periodic Potential Problem”. In: *Phys. Rev.* 94 (6 June 1954), pp. 1498–1524. DOI: [10.1103/PhysRev.94.1498](https://doi.org/10.1103/PhysRev.94.1498). URL: <http://link.aps.org/doi/10.1103/PhysRev.94.1498>.
- [121] L. I. Slepyan. *Models and phenomena in fracture mechanics*. New York, Berlin, Heidelberg: Springer, 2002.
- [122] S. B. Soffer. “Statistical Model for the Size Effect in Electrical Conduction”. In: *Journal of Applied Physics* 38.4 (1967), pp. 1710–1715. DOI: [10.1063/1.1709746](https://doi.org/10.1063/1.1709746). URL: <http://dx.doi.org/10.1063/1.1709746>.
- [123] S. B. Soffer. “Effect of Weak Surface Autocorrelation on the Size Effect in Electrical Conduction”. In: *Phys. Rev. B* 2 (10 Nov. 1970), pp. 3894–3898. DOI: [10.1103/PhysRevB.2.3894](https://doi.org/10.1103/PhysRevB.2.3894). URL: <https://link.aps.org/doi/10.1103/PhysRevB.2.3894>.
- [124] G. A. Somorjai and Y. Li. *Introduction to surface chemistry and catalysis*. John Wiley & Sons, 2010.
- [125] E. H. Sondheimer. “The Theory of the Transport Phenomena in Metals”. In: *Proceedings of the Royal Society of London A: Mathematical, Physical and Engineering Sciences* 203.1072 (1950), pp. 75–98. DOI: [10.1098/rspa.1950.0127](https://doi.org/10.1098/rspa.1950.0127). URL: <http://rspa.royalsocietypublishing.org/content/203/1072/75>.
- [126] E. Sondheimer. “The mean free path of electrons in metals”. In: *Advances in Physics* 1.1 (1952), pp. 1–42. DOI: [10.1080/00018735200101151](https://doi.org/10.1080/00018735200101151). URL: <http://dx.doi.org/10.1080/00018735200101151>.
- [127] R. Spadacini and G. Tommei. “A Markovian approach to atomic scattering from rough surfaces”. In: *Surface Science* 133.1 (1983), pp. 216–232. DOI: [http://dx.doi.org/10.1016/0039-6028\(83\)90492-2](https://doi.org/10.1016/0039-6028(83)90492-2). URL: <http://www.sciencedirect.com/science/article/pii/0039602883904922>.
- [128] C. Sprodzowski and K. Morgenstern. “Three types of bulk impurity induced interference patterns on the (100) and (111) faces of Ne- and Ar-doped silver”. In: *Phys. Rev. B* 82 (16 Oct. 2010), p. 165444. DOI: [10.1103/PhysRevB.82.165444](https://doi.org/10.1103/PhysRevB.82.165444). URL: <http://link.aps.org/doi/10.1103/PhysRevB.82.165444>.
- [129] M. Steslicka and B. Stankiewicz. “Localized states in a simple cubic crystal via the next-nearest neighbor approximation”. In: *International Journal of Quantum Chemistry* 12.3 (1977), pp. 433–441. DOI: [10.1002/qua.560120302](https://doi.org/10.1002/qua.560120302). URL: <http://dx.doi.org/10.1002/qua.560120302>.
- [130] T. Sun et al. “Surface and grain-boundary scattering in nanometric Cu films”. In: *Phys. Rev. B* 81 (15 Apr. 2010), p. 155454. DOI: [10.1103/PhysRevB.81.155454](https://doi.org/10.1103/PhysRevB.81.155454). URL: <http://link.aps.org/doi/10.1103/PhysRevB.81.155454>.
- [131] P. R. Surjan. *Second Quantized Approach to Quantum Chemistry: An Elementary Introduction*. 1st ed. Springer-Verlag Berlin Heidelberg, 1989.

- [132] N. Tao. “Electron transport in molecular junctions”. In: *Nature nanotechnology* 1.3 (2006), pp. 173–181.
- [133] V. M. Tapilin. “On the calculation of the electronic structure of a semi-infinite crystal in the LMTO-tight-binding approximation”. In: *Surface Science* 206 (1988), pp. 405–412.
- [134] V. M. Tapilin. “Modified tight-binding equations for wave functions of semi-infinite crystals and interfaces”. In: *Phys. Rev. B* 52 (19 Nov. 1995), pp. 14198–14205. DOI: [10.1103/PhysRevB.52.14198](https://doi.org/10.1103/PhysRevB.52.14198). URL: <http://link.aps.org/doi/10.1103/PhysRevB.52.14198>.
- [135] C. R. Tellier and A. J. Tossier. “Size Effects In Electrical Conductivity”. In: *Size Effects in Thin Films*. Ed. by C. Tellier and A. Tossier. Thin Films Science and Technology. Oxford: Elsevier, 1982, pp. 1–151. DOI: <http://dx.doi.org/10.1016/B978-0-444-42106-7.50005-X>. URL: <http://www.sciencedirect.com/science/article/pii/B978044442106750005X>.
- [136] J. Thomson. “On the theory of electric conduction through thin metallic films”. In: *Proc. Camb. Phil. Soc.* 11 (1901), p. 120.
- [137] N. Trivedi and N. W. Ashcroft. “Quantum size effects in transport properties of metallic films”. In: *Phys. Rev. B* 38 (17 Dec. 1988), pp. 12298–12309. DOI: [10.1103/PhysRevB.38.12298](https://doi.org/10.1103/PhysRevB.38.12298). URL: <http://link.aps.org/doi/10.1103/PhysRevB.38.12298>.
- [138] P. Wahl et al. “Quantum Coherence of Image-Potential States”. In: *Phys. Rev. Lett.* 91 (10 Sept. 2003), p. 106802. DOI: [10.1103/PhysRevLett.91.106802](https://doi.org/10.1103/PhysRevLett.91.106802). URL: <http://link.aps.org/doi/10.1103/PhysRevLett.91.106802>.
- [139] R. F. Wallis. “Effect of Free Ends on the Vibration Frequencies of One-Dimensional Lattices”. In: *Physical Review* 105 (2 Jan. 1957), pp. 540–545. DOI: [10.1103/PhysRev.105.540](https://doi.org/10.1103/PhysRev.105.540). URL: <http://link.aps.org/doi/10.1103/PhysRev.105.540>.
- [140] Z. L. Wang. “Dynamic Elastic Electron Scattering I: Bloch Wave Theory”. In: *Elastic and Inelastic Scattering in Electron Diffraction and Imaging*. Boston, MA: Springer US, 1995, pp. 23–60. DOI: [10.1007/978-1-4899-1579-5_2](https://doi.org/10.1007/978-1-4899-1579-5_2). URL: http://dx.doi.org/10.1007/978-1-4899-1579-5_2.
- [141] M. Watanabe. “Elastic scattering of the conduction electrons by adsorbed hydrogen”. In: *Surface Science* 34.3 (1973), pp. 759–772. DOI: [http://dx.doi.org/10.1016/0039-6028\(73\)90042-3](http://dx.doi.org/10.1016/0039-6028(73)90042-3). URL: <http://www.sciencedirect.com/science/article/pii/0039602873900423>.
- [142] M. Watanabe. “The Elastic Scattering of the Conduction Electrons by Oxygen Adsorbed on Pt Wire”. In: *Japanese Journal of Applied Physics* 13.S2 (1974), p. 149. URL: <http://stacks.iop.org/1347-4065/13/i=S2/a=149>.

- [143] M. Watanabe. “Interaction between adsorbed atoms and conduction electrons of thin evaporated films”. In: *Thin Solid Films* 36.1 (1976), pp. 65–70. DOI: [http://dx.doi.org/10.1016/0040-6090\(76\)90403-X](http://dx.doi.org/10.1016/0040-6090(76)90403-X). URL: <http://www.sciencedirect.com/science/article/pii/004060907690403X>.
- [144] P. Wißmann and H.-U. Finzel. *Electrical Resistivity of Thin Metal Films*. 1st ed. Springer Tracts in Modern Physics 223. Springer-Verlag Berlin Heidelberg, 2007.
- [145] H. Ou-Yang, B. Källebring, and R. Marcus. “Surface properties of solids using a semi-infinite approach and the tight-binding approximation”. In: *The Journal of chemical physics* 98.9 (1993), pp. 7405–7411.
- [146] J. Ziman. *Electrons and Phonons: The Theory of Transport Phenomena in Solids*. International series of monographs on physics. OUP Oxford, 1960.
- [147] J. Ziman. “The calculation of Bloch functions”. In: *Solid State Physics* 26 (1971), pp. 1–101.

A Auxiliary expressions

A.1

Following [107], the discrete Fourier transform [49] $\psi_y^F : \mathbb{C} \rightarrow \mathbb{C}$ of $\{\psi_{x,y}\}_{x \in \mathbb{Z}}$ (along the x axis) is defined by

$$\begin{aligned} \psi_y^F &= \psi_{y,+} + \psi_{y,-}, \text{ where} \\ \psi_{y,+}(z) &= \sum_{x=0}^{+\infty} \psi_{x,y} z^{-x}, \psi_{y,-}(z) = \sum_{x=-\infty}^{-1} \psi_{x,y} z^{-x}. \end{aligned} \quad (\text{A.1})$$

The discrete Fourier transform ψ_y^{sF} of the sequence $\{\psi_{x,y}^s\}_{x \in \mathbb{Z}}$ is well defined for $y \geq 1$, using which the discrete Helmholtz equation (1.6a), for all y away from the boundary, is expressed (recollected from [107]) as

$$Q\psi_y^{sF} = \psi_{y+1}^{sF} + \psi_{y-1}^{sF}, \quad (\text{A.2a})$$

$$\text{where } Q(z) := -z - z^{-1} - \beta^{-1}\mathcal{E}_\kappa, \quad (\text{A.2b})$$

$$\lambda := \frac{r - \hbar}{r + \hbar}, \hbar := \sqrt{\mathcal{H}}, r := \sqrt{\mathcal{R}}, \quad (\text{A.2c})$$

$$\mathcal{H} := Q - 2, \mathcal{R} := Q + 2. \quad (\text{A.2d})$$

The complex functions $\hbar, r, \mathcal{H}, \mathcal{R}$, and λ are defined on $\mathbb{C} \setminus \mathcal{B}$ where \mathcal{B} denotes the union of branch cuts for λ , borne out of the chosen branch $-\pi < \arg \mathcal{H}(z) < \pi, \Re \hbar(z) > 0, \Re r(z) > 0, \text{sgn} \Im \hbar(z) = \text{sgn} \Im r(z)$, for \hbar and r such that $|\lambda(z)| \leq 1, z \in \mathbb{C} \setminus \mathcal{B}$, as $\Im \mathcal{E}_\kappa$ in (A.2c) is positive. The general solution of (A.2a) is given by the expression

$$\psi_y^{sF} = c_1 \lambda^y + c_2 \lambda^{-y}, \quad (\text{A.3})$$

where $c_{1,2}$ are arbitrary analytic functions of z in \mathcal{A} (to be specified later).

A.2

Following [112], using the discrete Fourier transform defined by (A.1), the discrete Helmholtz equation (2.3) can be expressed as (A.2a) for all $y \in \mathbb{Z}$ inside the lattice but away from the boundary, where

$$Q(z) := \frac{\frac{3}{2} - z^2 - z^{-2} - \frac{3}{2}\beta^{-1}\mathcal{E}_\kappa}{z + z^{-1}}, z \in \mathbb{C}. \quad (\text{A.4})$$

The general solution is again given by the expression (A.3) (using (A.2c)) but with Q given by (A.4). The zeros of \mathcal{H} are $z_{\hbar}, z_{\hbar a}, 1/z_{\hbar}$, and $1/z_{\hbar a}$, where

$$z_{\hbar} = \frac{1}{4}(-2 + \sqrt{6}\sqrt{3 - \beta^{-1}\mathcal{E}_\kappa} - \sqrt{6(1 - \beta^{-1}\mathcal{E}_\kappa) - 4\sqrt{6}\sqrt{3 - \beta^{-1}\mathcal{E}_\kappa}}), \quad (\text{A.5a})$$

$$\text{and } z_{\hbar a} = \frac{1}{4}(-2 - \sqrt{6}\sqrt{3 - \beta^{-1}\mathcal{E}_\kappa} + \sqrt{6(1 - \beta^{-1}\mathcal{E}_\kappa) + 4\sqrt{6}\sqrt{3 - \beta^{-1}\mathcal{E}_\kappa}}), \quad (\text{A.5b})$$

and these four points in \mathbb{C} are also the branch points of \hbar . Due to the property $\mathcal{R}(z) = -\mathcal{H}(-z)$, the zeros of \mathcal{R} are related to those of \mathcal{H} through multiplication by -1 . The zeros of \mathcal{R} are $z_r (= -z_{\hbar}), z_{ra} (= -z_{\hbar a}), 1/z_r (= -1/z_{\hbar})$, and $1/z_{ra} (= -1/z_{\hbar a})$ and these four points are also the branch points of r . Note that the square root in the expression for z_{\hbar} and $z_{\hbar a}$ is chosen such that z_{\hbar} and $z_{\hbar a}$ lie inside the unit circle \mathbb{T} (since it is assumed that $\Im\mathcal{E}_\kappa > 0$).

B Multiplicative factorization of kernel

The multiplicative factorization of \mathcal{L} is [84]

$$\mathcal{L}(z) = \mathcal{L}_+(z)\mathcal{L}_-(z), z \in \mathcal{A}_L, \quad (\text{B.1a})$$

where the factors \mathcal{L}_{\pm} are given by

$$\mathcal{L}_{\pm}(z) = \exp\left(\pm \frac{1}{2\pi i} \oint_{\mathcal{C}} \frac{\log \mathcal{L}(\zeta)}{z - \zeta} d\zeta\right), z \in \mathbb{C} \quad (\text{B.1b})$$

such that $|z| \gtrless R_L^{\pm 1}$.

In (B.1b), \mathcal{C} is any rectifiable, closed, counterclockwise contour lying in annulus of analyticity \mathcal{A} for \mathcal{L} . Also it is implicitly assumed that $\mathcal{L}_{\pm}(z) = \mathcal{L}_{\mp}(z^{-1})$, allowing the representation to be unique [84]. Notice that the function \mathcal{L}_+ (resp. \mathcal{L}_-) is analytic, in fact it has neither poles nor zeros, in the exterior (resp. interior) of a disk centered at 0 in \mathbb{C} with radius R_L (resp. R_L^{-1}).

C Auxiliary details for the geometric part of the solution

The geometric part of the solution modulo the incident wave (1.5) can be constructed using the incident wave and reflected wave in the ‘bulk’ lattice

$$\psi_{\mathbf{x},\mathbf{y}}^{\text{incr}} = \psi_{\mathbf{x},\mathbf{y}}^{\text{inc}} + c\psi_{\mathbf{x},\mathbf{y}}^r, \mathbf{x} \in \mathbb{Z}, \mathbf{y} \in \mathbb{Z}^+, \quad (\text{C.1})$$

where c is needed to be determined. Since, it is required that $\psi_{\mathbf{x},\mathbf{y}}^{\text{incr}} = 0$ at $\mathbf{y} = 1, \mathbf{x} < 0$, or $\mathbf{y} = 0, \mathbf{x} \geq 0$, $\psi_{\cdot,0}^r = -\psi_{\cdot,0}^{\text{inc}}$. Thus,

$$\psi_{\mathbf{x},\mathbf{y}}^{\text{incr}}(s) = A e^{-i\kappa_x \mathbf{x} - i\kappa_y \mathbf{y}} - A \begin{cases} e^{-i\kappa_x \mathbf{x} + i\kappa_y \mathbf{y}} & \text{for } s = A, \\ e^{-i\kappa_x \mathbf{x} + i\kappa_y (\mathbf{y}-2)} & \text{for } s = B, \end{cases} \quad (\text{C.2})$$

for all $\mathbf{x} \in \mathbb{Z}, \mathbf{y} \in \mathbb{Z}^+$, where $s = A$ corresponds to the right side of step while $s = B$ corresponds to the left side of step. Suppose $\theta = \theta_r$ corresponds to the angle of ray emanating from the reflected waves from the right side of the step. Then, it is easy to see that

$$\psi_{\mathbf{x},\mathbf{y}}^g = \psi_{\mathbf{x},\mathbf{y}}^{\text{incr}}(A)H(\theta_r - \theta) + \psi_{\mathbf{x},\mathbf{y}}^{\text{incr}}(B)H(\theta - \theta_r). \quad (\text{C.3})$$

Note that $\psi_{\mathbf{x},\mathbf{y}}^g = \sum_{s=A,B} \psi_{\mathbf{x},\mathbf{y}}^s |_{P_s}$ as the second term that appears in the far-field approximation (4.2a).

D Auxiliary details for the exact solution

D.1

It follows from (1.5), (1.11a), after applying the multiplicative factorization $\mathcal{L} = \mathcal{L}_+ \mathcal{L}_-$, that $\mathcal{L}_+ \psi_{2,+}^s + \mathcal{L}_-^{-1} \psi_{2,-}^s = C(z), z \in \mathcal{A}$ where

$$C(z) = (\mathcal{L}_-^{-1} - \mathcal{L}_+) (w - Q A e^{-i\kappa_y} \delta_{D-} (z z_P^{-1} e^{-\epsilon}) - A \delta_{D+} (z z_P^{-1} e^{+\epsilon}), \quad z \in \mathcal{A}. \quad (\text{D.1a})$$

Hence,

$$\begin{aligned} C_{\pm}(z) &= \mp \psi_{-1,1}^s \mathcal{L}_{\pm}^{\pm 1}(z) \pm z \psi_{0,1}^s (\mathcal{L}_{\pm}^{\pm 1}(z) - l_{+0}) \\ &\quad \pm A e^{-i\kappa_y} \delta_{D-} (z z_P^{-1} e^{-\epsilon}) \\ &= (Q(z) \mathcal{L}_{\pm}^{\pm 1}(z) - \mathcal{L}_+(z_P) Q(z_P) + l_{+0}(z - z_P)) \\ &\quad \mp (\mathcal{L}_-^{-1}(z_P) - \mathcal{L}_{\pm}^{\pm 1}(z)) A \delta_{D+} (z z_P^{-1} e^{+\epsilon}), \end{aligned} \quad (\text{D.1b})$$

where $l_{+0} = \lim_{z \rightarrow \infty} \mathcal{L}_+(z)$. In (D.1b), \pm signs concur. After an application of the Liouville theorem [84, 107], in terms of the one-sided discrete Fourier transform the complex function $\psi_{2,\pm}^s$ is given by

$$\psi_{2,\pm}^s(z) = C_{\pm}(z) \mathcal{L}_{\pm}^{\mp 1}(z), z \in \mathbb{C}, |z| \gtrsim \max_{\min} \{R_{\pm}, R_{L_{\pm}}^{\pm 1}\}. \quad (\text{D.2})$$

Note that z_q and z_q^{-1} are the two zeros of Q (with $|z_q| < 1$), i.e., $Q(z) = z_q^{-1}(1 - z_q z)(1 - z_q z^{-1}) = -z^{-1}(z - z_q)(z - z_q^{-1})$; $Q_{\pm}(z) = z_q^{-1/2}(1 - z_q z^{\mp 1})$.

D.2

It follows from (1.5), (2.5), after applying the multiplicative factorization $\mathcal{L}Ntg = \mathcal{L}Ntg_+ \mathcal{L}Ntg_-$, that $(z + z^{-1})\mathcal{L}Ntg_+ \psi_{2;+}^s + (z + z^{-1})\psi_{2;-}^s \mathcal{L}Ntg_-^{-1} = C(z)$, $z \in \mathcal{A}$ where

$$\begin{aligned} C(z) &= (\mathcal{L}Ntg_-^{-1} - \mathcal{L}_+) (w - (-zu_{0,0}^{\text{inc}} + u_{-1,0}^{\text{inc}}) \\ &\quad - (z + z^{-1})Q(z)Ae^{-i\kappa_y} \delta_{D-}(zz_P^{-1}e^{-\epsilon}) \\ &\quad - (z + z^{-1})A\delta_{D+}(zz_P^{-1}e^{+\epsilon})), \quad z \in \mathcal{A}. \end{aligned} \tag{D.3a}$$

Using the detailed expressions provided by [112] for the infinite lattice (the expression for C_{\pm} can be also identified with (B.4) of [112]), as well as by [112] for the rigid constraint induced bifurcated waveguides' problem,

$$\begin{aligned} C_{\pm}(z) &= \mp z^2(-\psi_{0,1}^s)(\mathcal{L}_{\pm}^{\pm 1}(z) - l_{+0} - l_{+1}z^{-1}) \\ &\quad \mp z(-\psi_{1,1}^s - \psi_{0,2}^s)(\mathcal{L}_{\pm}^{\pm 1}(z) - l_{+0}) \\ &\quad \mp (-Ae^{-i\kappa_y} z_P^{-2} + \psi_{-1,2}^s)(\mathcal{L}_{\pm}^{\pm 1}(z) - \bar{l}_{-0}) \\ &\quad \mp z^{-1}(-Ae^{-i\kappa_y} z_P^{-1})(\mathcal{L}_{\pm}^{\pm 1}(z) - \bar{l}_{-0} - \bar{l}_{-1}z) \\ &\quad \quad \pm Ae^{-i\kappa_y}(\bar{l}_{-0}(z^{-1} + z_P^{-1}) + \bar{l}_{-1})z_P^{-1} \\ &\quad \pm Ae^{-i\kappa_y} \delta_{D-}(zz_P^{-1}e^{-\epsilon})(\mathcal{L}_{\pm}^{\pm 1}(z)(z + z^{-1})Q(z) \\ &\quad - \mathcal{L}_+(z_P)(z_P + z_P^{-1})Q(z_P) + l_{+0}(z^2 - z_P^2) + l_{+1}(z - z_P)) \\ &\quad \mp z(-\psi_{0,2}^{\text{inc}})(\mathcal{L}_{\pm}^{\pm 1}(z) - l_{+0}) + \psi_{-1,2}^{\text{inc}}(\mathcal{L}_{\pm}^{\pm 1}(z) - \bar{l}_{-0}) \\ &\quad \quad \pm A\delta_{D+}(zz_P^{-1}e^{+\epsilon})(\mathcal{L}_{\pm}^{\pm 1}(z)(z + z^{-1}) \\ &\quad - \mathcal{L}_-^{-1}(z_P)(z_P + z_P^{-1}) - l_{+0}(z - z_P) - \bar{l}_{-0}(z^{-1} - z_P^{-1})), \end{aligned} \tag{D.3b}$$

where $l_{+0} = \lim_{z \rightarrow \infty} \mathcal{L}_+(z)$, $l_{+1} = \lim_{z \rightarrow \infty} z(\mathcal{L}_+(z) - l_{+0})$, $\bar{l}_{-0} = \lim_{z \rightarrow 0} \mathcal{L}_-^{-1}(z)$, etc. Then

$$\begin{aligned} J(z) &= ((z + z^{-1})\mathcal{L}_+(z)\psi_{2;+}^s(z) + \bar{l}_{-0}\psi_{-1,2}^s \\ &\quad - z l_{+0}\psi_{0,2}^s) - C_+(z) \\ &= -\frac{z + z^{-1}}{\mathcal{L}_-(z)}\psi_{2;-}^s(z) + C_-(z) + \bar{l}_{-0}\psi_{-1,2}^s \\ &\quad - z l_{+0}\psi_{0,2}^s \text{ on } \mathcal{A}, \end{aligned} \tag{D.4}$$

holds. Notice that as $z \rightarrow \infty$, $J(z) \sim \text{constant}$, on the other hand, as $z \rightarrow 0$, $J(z) \sim C_-(0)$, where $C_-(0) = 0$. The function $C_+(z)$ (resp. $C_-(z)$) is analytic at $z \in \mathbb{C}$ such that $|z| > \max\{R_+, R_L\}$ (resp. $|z| < \min\{R_-, R_L^{-1}\}$). In (D.3b), \pm signs concur. By an application of the Liouville's theorem, the solution of

the discrete Wiener–Hopf equation (2.5) can be written in terms of one-sided discrete Fourier transforms as

$$(z + z^{-1})\psi_{2;\pm}^s(z) = \mathcal{L}_{\pm}^{\mp 1}(z)(\pm z l_{+0}\psi_{0,2}^s \mp \bar{l}_{-0}\psi_{-1,2}^s + C_{\pm}(z)), z \in \mathbb{C}, |z| \geq \frac{\max\{R_{\pm}, R_L^{\pm 1}\}}{\min\{R_{\pm}, R_L^{\pm 1}\}}. \quad (\text{D.5})$$

Substituting (D.5) in (2.4a), the expression for $\psi_{1,+}^s$, in terms of $\psi_{0,1}^s, \psi_{1,1}^s, \psi_{0,2}^s$ and $\psi_{-1,2}^s$, is found, it is further simplified to obtain $\psi_{0,1}$ which is similar to the expression found by [112]. In particular, using the residue calculus, $\psi_{0,1}$ is obtained as

$$\begin{aligned} \psi_{0,1} = & -Ae^{-i\kappa_y} \frac{\mathcal{L}_+(z_P)(z_P + z_P^{-1})Q(z_P)}{((z_P + z_q^{-1})l_{+0} + l_{+1})(z_P - z_q^{-1})} \\ & - A \frac{1 - z_q^2 z_P^{-2}}{Q(z_P)} \frac{z_P + z_q^{-1}}{\mathcal{L}_-(z_P)} \frac{1}{(z_P + z_q^{-1})l_{+0} + l_{+1}}. \end{aligned} \quad (\text{D.6a})$$

Further, $l_{+1} = 0$ due to the presence of even powers of z in the kernel (an indirect consequence of the double degeneracy of energy band relation of \mathfrak{R} since it is a union of two decoupled lattices \mathfrak{T} and the replicated \mathfrak{T}^{R}). Hence,

$$\begin{aligned} \psi_{0,1} = & A \frac{(1 - z_q^2 z_P^{-2})}{l_{+0}} \left(e^{-i\kappa_y} \mathcal{L}_+(z_P) \right. \\ & \left. - \frac{1}{Q(z_P)} \mathcal{L}_-(z_P) \right). \end{aligned} \quad (\text{D.6b})$$

Above expression can also be compared with mathematically analogous problems studied by [116] for the square lattice half-planes with a different set of boundary conditions. By translational symmetry $\psi_{1,1}^s = e^{-i\kappa_x} \psi_{0,1}^s$, which is plotted in Fig. 10. Note that $(z + z^{-1})Q(z) = -z^{-2}(z^2 - z_q^2)(z^2 - z_q^{-2})$, so that $((z + z^{-1})Q)_{\pm}(z) = (-z_q)^{-1/2} z_q^{-1/2} (1 - z_q^2 z^{\mp 2})$.

E Auxiliary details for far-field approximation

E.1

Following [107], let $\xi_f = \mp \pi + \pi H(\beta^{-1}\mathcal{E}_{\kappa})H(4 - \beta^{-1}\mathcal{E}_{\kappa})$. Let the ‘‘polar’’ coordinates (R, θ) for $(\mathbf{x}, \mathbf{y}) \in \mathbb{Z}^2$, be specified by the relations

$$\begin{aligned} \mathbf{x} &= R \cos \theta, \mathbf{y} = R \sin \theta, \\ R &= \sqrt{\mathbf{x}^2 + \mathbf{y}^2} > 0, \theta \in [0, \pi). \end{aligned} \quad (\text{E.1})$$

The mapping $z = e^{-i\xi}$ and polar coordinates (R, θ) are used to rewrite the solution (3.2) as

$$\psi_{\mathbf{x},\mathbf{y}}^s = -\frac{1}{2\pi} \text{AC}_0 \int_{\mathcal{C}_{\xi}} \frac{\mathcal{K}(e^{-i\xi})e^{iR\Phi(\xi)}}{e^{i(\xi - \kappa_x)} - 1} e^{-in(\xi)} d\xi, \quad (\text{E.2})$$

where \mathcal{C}_ξ is a contour, traversed from ξ_i to ξ_f , in the strip $\mathcal{S} = \{\xi \in \mathbb{C} : \xi_1 \in [\xi_i, \xi_f], -\kappa_2 < \xi_2 < \kappa_2 \cos \Theta\}$, and

$$\begin{aligned}\phi(\xi) &= \eta(\xi) \sin \theta - \xi \cos \theta, \\ \eta(\xi) &= -i \log \lambda(e^{-i\xi}), \xi \in \mathcal{S}.\end{aligned}\tag{E.3}$$

The pole for the diffraction integral (E.2) (see [107] for details) is located on the contour of integration, \mathcal{C}_ξ , at $\xi = \kappa_x$ for all $\beta^{-1}\mathcal{E}_\kappa \in (-4, 0)$, or for all $\beta^{-1}\mathcal{E}_\kappa \in (0, 4)$ and admissible $\Theta \in [0, \pi/2]$, and at $\kappa_x + 2\pi$ for all $\beta^{-1}\mathcal{E}_\kappa \in (0, 4)$ and admissible $\Theta \in (\pi/2, \pi]$. The function ϕ (E.3) possesses a saddle point at $\xi = \xi_S$ on \mathcal{C}_ξ if [27, 29, 12] $\phi'(\xi_S) = \eta'(\xi_S) \sin \theta - \cos \theta = 0$, $\phi''(\xi_S) = \eta''(\xi_S) \sin \theta \neq 0$. The saddle point ξ_S for the diffraction integral (E.2) is same as that discussed in detail by [107]. The criterion for non-zero contribution of pole of diffraction integral (E.2) can be translated into a criterion that involves θ and Θ using the fact that ξ_S varies monotonically with θ (Theorem 3.4, [107]). See Fig. 5.1 in [107], where an illustration is provided for some values of $\beta^{-1}\mathcal{E}_\kappa$ of the dependence of θ_r on Θ , i.e., θ - Θ relation corresponding to the coalescence of pole and saddle point of diffraction integral $\kappa_x = \xi_S$ for $\beta^{-1}\mathcal{E}_\kappa \in (-4, 0)$ and $\beta^{-1}\mathcal{E}_\kappa \in (0, 4)$.

E.2

Suppose the polar coordinates (R, θ) are specified by the relations

$$\begin{aligned}\mathbf{x} &= 2R \cos \theta, \mathbf{y} = \frac{2}{\sqrt{3}}R \sin \theta, \\ \text{and } R &= \sqrt{\frac{1}{4}\mathbf{x}^2 + \frac{3}{4}\mathbf{y}^2} > 0, \theta \in [0, \pi).\end{aligned}\tag{E.4}$$

For $\beta^{-1}\mathcal{E}_\kappa \in (-3, 7/3) \cup (16/3, 6)$, the analysis of asymptotic approximation [12] of the scattered wavefunction in far field follows [112]. Let $\xi_{i_f} = \mp\pi$. Using $z = e^{-i\xi}$ and the polar coordinates (E.4), the solution (3.2) is rewritten as (E.2) where

$$\phi(\xi) = 2\left(\frac{1}{\sqrt{3}}\eta(\xi) \sin \theta - \xi \cos \theta\right),\tag{E.5}$$

η is given by (E.3)₂ and \mathcal{C}_ξ is a contour, traversed from ξ_i to ξ_f , in the strip $\mathcal{S} = \{\xi \in \mathbb{C} : \xi_1 \in [\xi_i, \xi_f], -\frac{1}{2}\kappa_2 < \xi_2 < \frac{1}{2}\kappa_2 \cos \Theta\}$. The pole for the diffraction integral (E.2) is located close to the contour of integration, \mathcal{C}_ξ , at $\xi = \kappa_x$ for all $\beta^{-1}\mathcal{E}_\kappa \in (-3, 7/3)$, or for all $\beta^{-1}\mathcal{E}_\kappa \in (7/3, 3)$ and admissible $\Theta \in [0, \pi]$. For the crack problem, there are two poles located at $\xi = \kappa_x$ and $\xi = i \log(-e^{-i\kappa_x})$.